2011

Future potential net primary production trends of contiguous United States rangelands

Adam LaSalle Moreno
The University of Montana

FUTURE POTENTIAL NET PRIMARY PRODUCTION TRENDS OF CONTIGUOUS UNITED STATES RANGELANDS

By

Adam LaSalle Moreno

B.S. Computer Engineering, Oregon State University, Corvallis, Oregon, 2004

Thesis

Presented in partial fulfillment of the requirements for the degree of

Masters of Science

in Forest Ecology

The University of Montana, Missoula, MT

College of Forestry and Conservation

December 2011

Approved by:

Sandy Ross, Associate Provost for Graduate Education
Graduate School

Steve W. Running, Advisor
Department of Ecosystem and Conservation Sciences

Anna Klene

Department of Geography

Cory Cleveland

Department of Ecosystem and Conservation Sciences

Abstract

Moreno, Adam, M.S., Fall 2011 Forest Ecology

Future potential net primary production trends of contiguous United States rangelands

Advisor: Steve Running

Rangelands are an important ecosystem covering nearly 24% of the earth's terrestrial vegetation. Climate change is predicted to affect many of the factors that influence the production of rangeland vegetation. Understanding future trends and patterns in net primary production (NPP) requires projected potential NPP to better understand how rangelands will be affected by a changing climate.

Here, I used climate data projected from a global climate model (GCM) to drive the biogeochemical model (Biome-BGC) in an attempt to simulate future potential NPP trends in rangelands of the contiguous United States from 2001-2100 on a 100 km2 scale. In response to the simulated climate projections, I found an overall slight increase in potential NPP throughout time. However, these increases were not spatially consistent; in some areas, NPP decreased substantially. Biome-BGC found three distinct zones that have similar potential NPP trends and primary correlating climatic factors that drove these trends. The south western portion of the United States may see a decrease in NPP driven mostly by a decrease in moisture. This simulation indicates a rise in NPP in the Great Plains mostly from c4 grasses driven primarily by an increase in temperature. Furthermore, it projects little to no change in The Great Basin driven by a combination of a slight increase in precipitation and maximum temperature.

Table of Contents

TABLE OF FIGURES

Acknowledgements

I am very much in debt to Steve Running for opening the opportunity for me to study in his incredible lab. He is always easy to talk to, encouraging, and gives terrific device. I would also like to thank Matt Reaves for both the financial and scientific support without which this project would not have been possible. I have thoroughly enjoyed every meeting that I have had throughout my time here. A big thanks to my committee members Anna Klene and Cory Cleveland for all of the help with bringing this thesis to completion. Thank You to Maosheng Zhao for all of the technical scientific advice and code that was used in this thesis.

To all of my lab mates and staff in the Nummerical Terradynamic Simulation Group, you all have made my time here intellectually enriching and enjoyable. Special thanks to Ryan Anderson whose depth of knowledge in Biome-BGC is invaluable to the modeling community. Also thanks to Jared Oyler who has always been so willing to help with my work and share his own which made the creation of this study more robust and timely. Truly everyone's brilliance in this lab is both humbling and inspirational.

Thank you to all of my fellow graduate students and friends without whom I could not have made it through this process. Special thanks to Loretta Baker and Michael Sulock for reviewing my thesis and ironing out the final touches. Thanks to Jonathan Leff for the statistical advice. Through both tough times and good the community here in Missoula has done nothing but make my life better.

1 Introduction

Rangelands occupy about 24% of the earth's terrestrial vegetation (Sims and Risser 1999), including 31% of the United States terrestrial surface (Havstad 2009). Rangeland is defined as:

> "A land cover/use category on which the climax or potential plant cover is composed principally of native grasses, grass-like plants, forbs, or shrubs suitable for grazing and browsing, and introduced forage species that are managed like rangeland. This includes areas where introduced hardy and persistent grasses, such as crested wheatgrass, are planted and such practices as deferred grazing, burning, chaining, and rotational grazing are used, with little or no chemicals or fertilizer being applied. Grasslands, savannas, many wetlands, some deserts, and tundra are considered to be rangeland. Certain communities of low forbs and shrubs, such as mesquite, chaparral, mountain shrub, and pinyon-juniper are also included as rangeland" (USDA 2009).

Rangelands provide an array of ecosystem services such as wildlife habitat, domestic livestock forage, and watershed protection (Standiford 1993). Arid rangelands also play an important role in mitigating the effects of climate change by acting as carbon sinks. Though rangelands experience relatively low carbon fluxes in and out of the atmosphere compared to other biomes (Svejcar 1997) they cover such a vast area that small changes in per unit area flux can make a large difference in the overall global carbon cycle (Batjes, 1998; Sundquist, 1993). United States rangelands are capable of sequestering carbon at rates up to 50 Tg C /yr (Lal, 2004). With improved management U.S. rangelands could sequester an additional 0.7 Mg C/ha/yr, and losses of 0.8 Mg C/ha/yr could be avoided annually (Schuman 2002). This equates to a total of 62 MMg C/yr. (10^{12} g C = 1 Tg C) across the United States (Schuman 2002) of potential carbon sequestration.

Net primary production (NPP), the net amount of carbon captured by plants through photosynthesis and converted to biomass, is the initial step in the carbon cycle. Measuring NPP integrates many climatic, ecological, geochemical and human influences (Nemani 2003). NPP only takes into account photosynthesis and plant respiration and is the primary measure of the

productivity an ecosystem's vegetation. NPP is also the easiest metric of an ecosystem's production by which to validate one's model on a coarse scale because of products produced by the Global Primary Production Data Initiative (GPPDI) and sensors such as the Moderate Resolution Imaging Spectroradiometer (MODIS). Only at coarse scales, (e.g. continental to global), can one obtain a complete picture of how an entire ecosystem behaves for the purposes of studying environmental issues such as climate change, land-use change, fragmentation, and loss of biodiversity (Turner 1995). Therefore, it is essential to understand NPP trends and patterns across a landscape to gain an accurate insight on carbon fluxes between ecosystems vegetation and the atmosphere. Understanding NPP trends and patterns across a landscape allows the quantification of sustainability of ecosystem services and health especially under the influence of climate change. Satellite imagery and spatially explicit models are necessary to estimate NPP of rangelands due to the need to understand how NPP will change over large areas. Direct empirical measurements are not feasible because running plot-level experiments over the entire United States are prohibitive.

There is a need for more studies that project the impacts global climate change will have on the U.S.'s expansive rangelands due to their significant ecological and human importance (Baker 1993; Thornton 2009). Most studies on rangeland NPP focus on a site-specific scale which does not allow for analysis on landscape heterogeneity (Briske 2005). Values of NPP from historic simulations for rangelands of the southeastern United States range from 220 to 355 g $C/m^2/yr$. (Tian 2010). Observed satellite measurements of NPP in rangelands of the northwest have shown NPP values of -130 to 200 g $C/m^2/yr$. (Reeves 2001). Plot studies in Californian rangelands show a NPP range of 800 to 1100 g $C/m^2/yr$. (Houlton 2010). Contest winning yields in Iowa corn approach 1800 g $C/m^2/yr$. (Duvick 1999). However, these estimates may or may not apply at large scales, thus understanding NPP trends on the landscape scale is a

good metric of the sustainability and value of ecosystems services such as carbon sequestration, animal forage, and wildlife habitat (Briske 2005; Fox 2009; Costanza 2006; Costanza 1998).

Over the next century, projections show that there will be changes in the global carbon and nitrogen cycles as well as changes in climatic factors such as temperature and precipitation. By 2100, atmospheric CO_2 concentrations are predicted to raise from 394 ppm presently, to 540 – 970 ppm depending on future carbon emissions scenarios (IPCC 2001). Over the next 100 years terrestrial nitrogen deposition is predicted to rise from the current average of 25 - 40 Tg N/yr. to 60 – 80 Tg N/yr. globally (Lamarque 2005), over a 2-fold increase. Mean terrestrial surface temperatures are predicted to rise from 0.6 – 4.0°C by 2100 (IPCC 2007). Also, extreme precipitation events are expected to become more frequent throughout the 21st century (IPCC 2007). The change in climate that we may see could have profound impacts on rangeland productivity, as well as ecological and socio-cultural implications. Some of these changes, such as carbon concentrations, are projected to occur uniformly across large scales (Conway 1994). Others, such as temperature, will change along regional gradients. The last century saw a change in mean annual temperature that ranged spatially from -2°C to 2°C (Hansen 2001). Yet other future environmental changes, such as nitrogen deposition, vary widely by region. Nitrogen deposition can range spatially from 0.26 to 16.7 kg N/ha/yr. in the United States (Holland 2005). Similarly, precipitation saw a range of change in trajectory spatially from -40 to 40 % from the annual average (NOAA 2008). This spatial heterogeneity of factors that affect NPP can greatly alter the pattern of a landscape.

NPP of the United States rangelands is strongly influenced by precipitation. The influence precipitation has on rangeland NPP was shown by Sala's 1988 collection of 9500 sites throughout the United States, which determined production in grasslands is highly correlated with precipitation and water holding capacity (Sala 1988). Sala (1988) showed there is a

relatively strong linear correlation between annual precipitation and production with an $r^2 = 0.9$. Nitrogen is also a limiting factor for rangeland growth and associated NPP values which have been shown by various fertilization experiments (Buis 2009, Schlesinger 2000, Hunt 1988). For example, Hunt (1988) found that there was an 81% increase in plant production in prairie ecosystems in response to nitrogen fertilization. As a result, small changes in factors that influence rangeland NPP are thought to have a large impact on the overall carbon cycle and ecosystem services. The influence rangelands have on the overall global carbon cycle is due to the tremendous amount of land, 295 million hectares (Mitchell 2000), these ecosystems occupy (Schuman, 2002).

How rangeland NPP will react over time to the changes that are expected in climate, carbon, and nitrogen cycles is uncertain. For example, the effect of CO_2 fertilization is ambiguous (Luo 2004). In some studies increasing CO_2 to 680–720 ppm increased the productivity of shortgrass steppe by 95% (Morgan 2004), but reduced, or had no effect on, biomass of annual grassland (Shaw et al. 2002; Dukes et al. 2005). There is also the possibility that higher CO_2 concentrations will result in progressive nitrogen limitation (PNL) (Vitousek 1991). PNL refers to the phenomena whereby nitrogen becomes increasingly sequestered in organic matter due to the increased growth response from higher CO_2 concentration thus gradually reducing the available mineral nitrogen in the soil making uptake of N more difficult over time. Experiments show different levels of PNL depending on climatic factors, location, and vegetation type (Thornton 2007). Nitrogen deposition is expected to rise throughout the next century (Lamarque 2005) potentially offsetting the effect of PNL. CO_2 fertilization also affects water use within the plant. Increased CO_2 concentration can lower stomatal conductance (Field 1995, Wand 1995). Lower stomatal conductance can reduce transpiration and slow soil water depletion, increasing production on water limited biomes such as rangelands (Fredeen 1997; Owensby 1997,

Niklaus 1998, Morgan 2004, Grünzweig & Körner 2001, Polley 2002, Polley 2010). Coupled with a change in the amount of precipitation, CO_2 fertilization can have a large effect on production. However, change in precipitation will vary widely throughout the United States with some areas losing precipitation while others may gain (IPCC 2007). Increasing temperatures have mixed effects on rangeland NPP. Coughenour (1997) showed that NPP decreases under hotter conditions, but this effect may be reduced by higher CO_2 concentrations. Temperature also has an impact on the amount of water available for plant production and can both stimulate and inhibit microbes that make nitrogen available for plant use (Jonasson 1999). These examples of how climate change could affect NPP are all long-term experiments and are done using devices that can only cover a limited space or cover a large area for a short amount of time. Therefore, it is unknown how vegetation over a large area over a long time frame will react to an increase in CO_2, changes in nitrogen deposition, and a changing climate (Lou 2004) which is crucial knowledge so that land managers may prepare for the coming future.

To fulfill the need of understanding NPP response to climate change in United States rangelands, this study modeled temporally and spatially explicit projected potential NPP trends. The study focuses on all rangelands within the conterminous United States from 2001-2100 on a daily time steps at a 100 km^2 resolution. A new version of Biome-BGC (Running 1993) called Agro-BGC (Di Vittorio 2010) was used to produce the simulations. To drive this model PRISM (Daly 1997) historical climate data was used and data produced by the Model for Interdisciplinary Research on Climate version 3.2 (MIROC) was used to calculate future projections (K-1 2004, Nozawa 2007). A 10 km on a side cell size shows changes over a varying landscape related to orographic effects and major climatic patterns. Also, because of rangeland's low vegetative heterogeneity a 10x10 km scale will capture much of the effect from various vegetation types (Riera 1998). The objective of this study is to simulate trends in future potential

NPP and how the environmental changes may influence rangeland production spatially and temporally.

2 Methods

2.1 Overview

This study uses various data sets to drive simulations using the Agro-BGC version of Biome-BGC. As seen in Figure 2-1 this model requires a set of inputs and has several steps before a final model run can be completed. Inputs usually are not produced specifically for Biome-BGC so that for my use they must be manipulated to fit the Biome-BGC required input format.

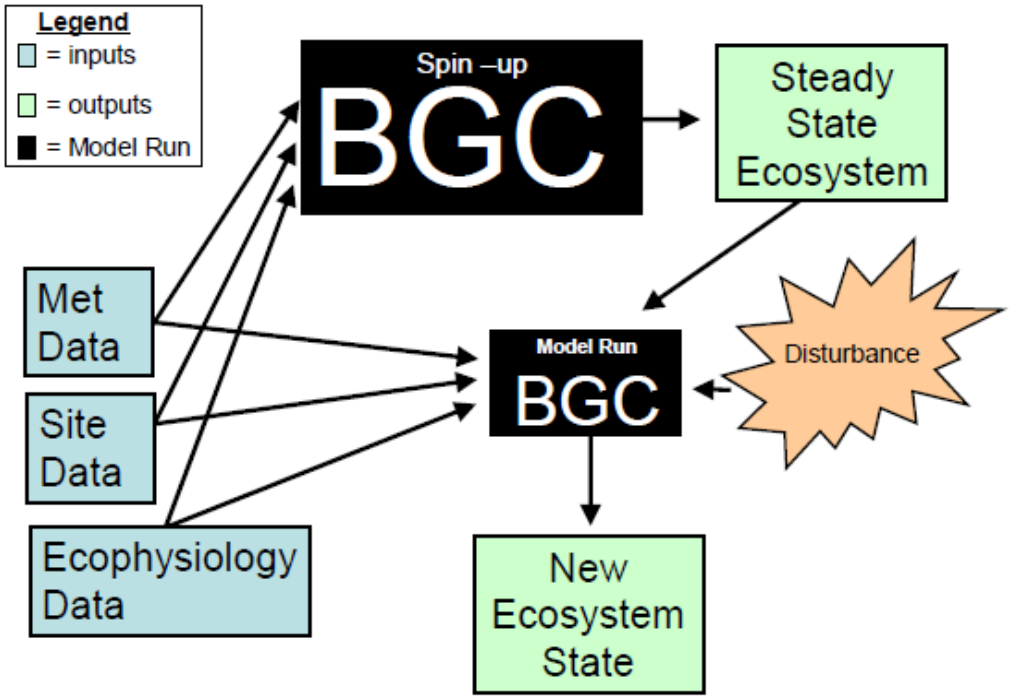

Figure 2-1. Conceptual diagram showing BiomeBGC's general model structure (Golinkoff 2010).

As part of the required inputs for Biome-BGC, parameterization of the physiology of cover types is needed. New parameters for shrub species were calibrated and then validated through literature (appendix). The calibrated parameters proved to be an improvement over the default shrub parameters when running simulations over a continental scale producing a more realistic extent of shrubs throughout the study area.

The study area contains all contiguous United States rangeland as defined by Reeves and Mitchell (2010). I used the Natural Resources Conservation Service's definition of rangeland in this study, as previously defined and distinguished shrub lands as containing more than 10% shrub cover.

First, scaling of input datasets was performed, I then ensured the downscaled data remained consistent with the original data set, and finally I started projection runs. These datasets were then scaled and masked to show only rangeland values of the United States. I compared the Biome-BGC outputs against two external empirical data sets for the first ten years of the projection to calculate the accuracy and bias of Biome-BGC outputs. The outputs were also analyzed to produce trends of NPP, as well as maps and histograms of major factors that influence these trends.

2.1.1 Biome-BGC

Biome-BGC is a mechanistic model that is used to estimate the state and fluxes of carbon, nitrogen, and water in an ecosystem (Golinkoff 2010). Biome-BGC is a "big leaf" model meaning that Biome-BGC does not simulate every individual life form within the ecosystem but instead considers all members of the ecosystem as one entity. To drive the simulations there are three files required: 1) a parameter file which describes the physiology and phenology of the biome to be simulated; 2) a climate file that provides the daily minimum temperature, maximum temperature, mean temperature, precipitation, vapor pressure deficit, day length, and incoming solar radiation; and 3) an initiation file that describes input and output files, soil data, and how the simulation should be run. To complete a full simulation, a spin-up run is required before the desired projection run can be initiated. The spin-up allows Biome-BGC to run until a steady state of soil carbon is reached in the ecosystem, which produces initial conditions for the projection's run. Spin-ups and their corresponding projection simulations

must be performed for every cover type within the cell. The need to run separate simulations for each cover type is due to the fact that each cover type will use different parameter files and Biome-BGC doesn't allow for multiple cover types within the same simulation.

2.1.2 Study area and spatial setup

Biome-BGC is a point model with no "neighboring effects", meaning cells do not affect one another and are simulated independently. A simulation that covers various cells in Biome-BGC requires the creation of an organizational structure of folders that contain information on every cell that will be modeled. I used a raster image to create a grid that represents every terrestrial cell in the conterminous United States at a 10 km resolution. Every folder in the grid contains initiation files for spin-ups and projection runs for every cover type as well as all outputs from each simulation.

Downscaling of the data and creation of the spatial gridding data structure was done simultaneously. To set up a spatial gridding for Biome-BGC every cell used the same parameter files that describe the physiology of the biome type and CO_2 concentrations. However, each cell used different historical and projected climatology, soil, and nitrogen deposition data. I wrote a program in python to perform all of the tasks of calculating the missing climatology variables. The task that the program performed were downscaling the climatology temporally, converting data to Biome-BGC input format, setting up the gridded organizational structure, manipulating the initiation files for both the spin-up and the projection runs for each cover type, and modifying each file to contain the appropriate soil data, nitrogen deposition file pointer, CO_2 concentration file pointer, and land-cover type parameter file pointer. Figure 2-2 and Figure 2-3 show the area of extent of rangeland that was analyzed. There are two rangeland maps, one for shrubs and one for herbs. The maps show the percentage of each respective cover type's ground cover within each cell produced by Reeves et.al. (2010). The percentages of cover type on the land were then used

to scale the final NPP for each cell. The cover types focused on in this study are shrubs, C3 and C4 grasses because these vegetation types make up the vast majority of rangeland plant life as outlined in the definition of rangeland that I used in this study.

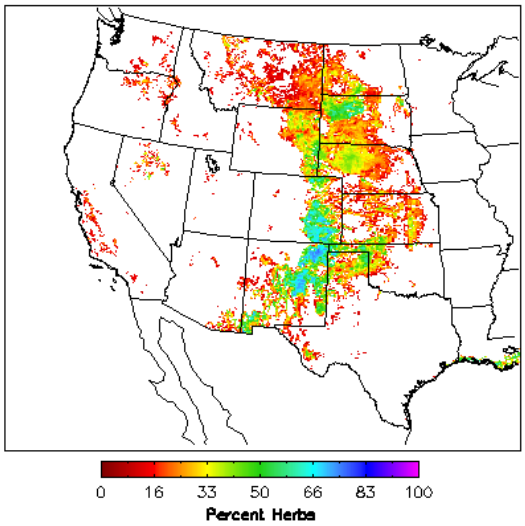

Figure 2-2. Percent cover of combined C3 and C4 of United States rangelands.

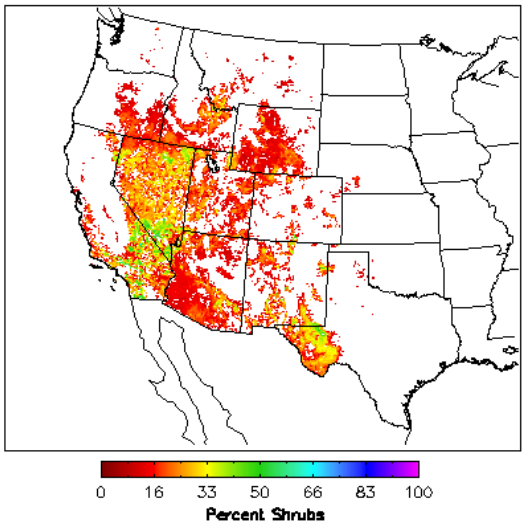

Figure 2-3. Percent cover of shrubs of United States rangelands.

According to these maps, shrubs and grasses are generally located in different areas and will produce distinctly different results spatially when simulated. Grasslands are mainly distributed east of the Rocky Mountain Front with the highest percentage lying in the Texas, Colorado, New Mexico, Kansas, and Oklahoma regions. Shrub lands principally lie in the southwest, with the highest percentage lying in California, Nevada, and Texas.

2.2 Climatology

2.2.1 PRISM

Spin-up simulation runs were performed before our desired simulations to obtain initial conditions for our simulation. These simulations were run until the soil carbon reached a point of steady state. These spin-ups required climate data provided by PRISM (Daly 2001) and dates chosen for spin-ups were from 1940 to 2001 because of data availability. PRISM data resolution is in 100 km^2 cells, the base resolution selected for this study, thus allowing for direct application without the need for spatial downscaling.

2.2.2 GCM data

Meteorological data records, used to support forecasting analyses, were produced by the Model for Interdisciplinary Research on Climate version 3.2(MIROC) Global Climate Model (GCM) (K-1 2004, Nozawa 2007) and were used in conjunction with the IPCC CO_2 emissions scenario A1B and were spatially downscaled by Coulson et al. (2010). Performance of MIROC GCM data is assumed sufficient because studies have already verified validity of the MIROC GCM data (K-1 2004, Nozawa 2007) and because of its use by the IPCC 4^{th} assessment (2007). MIROC was chosen because of its data availability and that the scale matched the scale that was needed to perform this study. The scenario A1B is often thought of as a "middle of the road" scenario in regards to CO_2 emissions and is defined as:

> "A future world of very rapid economic growth, low population growth and rapid introduction of new and more efficient technology. Major underlying themes are economic and cultural convergence and capacity building, with a substantial reduction in regional differences in per capita income. In this world, people pursue personal wealth rather than environmental quality." (Solomon 2007).

Data was taken to cover the contiguous United States from the year 2001 to 2100. The original data sets were given at 10 km^2 cell resolution using monthly time steps.

2.2.3 Downscaling

For both the spin up and projection simulations, Biome-BGC requires daily time steps. Therefore temporal downscaling was necessary to adjust the data from monthly to daily time steps. To downscale the data temporally the delta method was used (Climate Impacts Group 2009). One year was chosen as the base year to retain daily variations in climate that get smoothed when the delta method is used implementing a multi-year average. From the years 2000-2006 in the surface observations gridding system data set (SOGS) (Jolly 2004), the year 2006 was chosen as the base year because this year has a total annual NPP closest to the multi-year mean. Because I used one year's daily patterns as a base, there will be a repeating temporal pattern throughout the entire simulation. In a particular cell, if SOGS has determined that there is a large rain event on a given day of the year there will always be a large rain event on this day for every year of the spin up and projection simulations.

To downscale both the GCM and PRISM data sets, first the SOGS 2006 daily data was aggregated to monthly time steps via a simple monthly mean (Figure 2-4). The monthly means were then used to calculate a scaling ratio for every month for every climate variable. During every month of the year, data from the PRISM and GCM data sets for each variable were used along with the SOGS 2006 monthly data to calculate a scaling ratio:

$$\frac{SOGS\ monthly\ data}{GCM\ (or\ PRISM) monthly\ data}$$

We manipulated the daily SOGS data with the appropriate monthly scaling ratio to adjust the difference between the SOGS data and the GCM or PRISM data (Figure 2-5). The goal was to achieve the same monthly average of the GCM and PRISM data while maintaining the daily

temporal pattern of the SOGS data set (as shown in Figure 2-6). Computationally, for temperature all calculations were done in Kelvin and then converted back to Celsius.

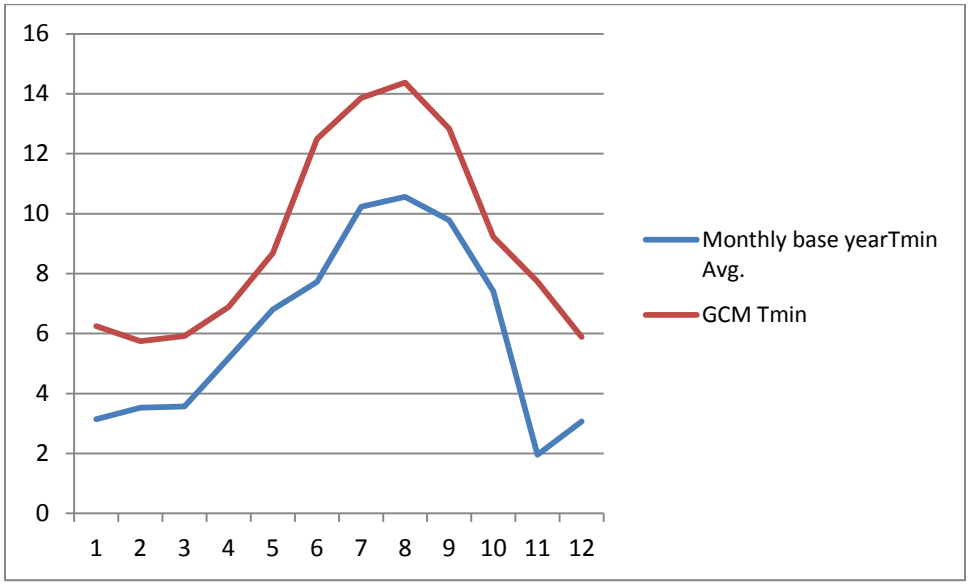

Figure 2-4 Example of GCM minimum temperature averages plotted with the SOGS monthly mean for one sample year in one sample location from the United States rangelands.

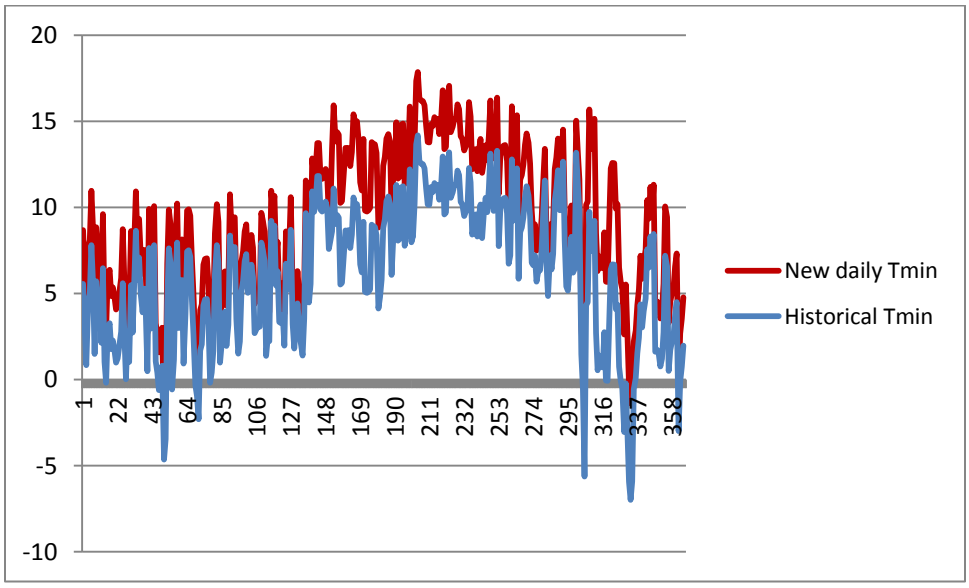

Figure 2-5 SOGS historic minimum temperature data vs. scaled minimum temperature data for one year after temporal downscaling. Daily pattern was the same but every monthly average was adjusted to match GCM (or PRISM) monthly means, thus the scaling was different for every month.

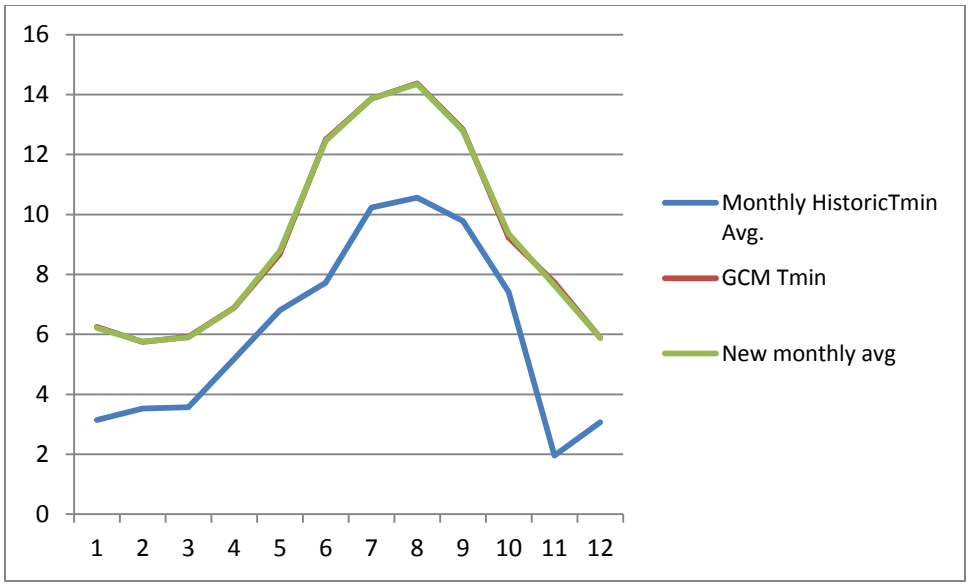

Figure 2-6 GCM monthly means ploted with the SOGS monthly mean and newly scaled monthly mean. The new monthly means were ploted exactly over the GCM curve illustrating that although daily patterns follow the SOGS daily pattern, the monthly means exactly matched the GCM monthly means.

After temporal downscaling was performed, I expected to see that the spatial and daily patterns matched those of the 2006 SOGS maps. Figure 2-7 shows that the magnitude of the MIROC daily rain events were different from the SOGS daily rain events due to the scaling which was desired because the magnitude of the MIROC rain events were adjusted by a multiplier that was calculated for every month. In this instance, the historical PRISM data shows higher rainfall for most months than the SOGS 2006 dataset for the same location. This same pattern is shown in the GCM scaled data. If there is no rain in the GCM or PRISM data for a given month then a negligible amount was added to maintain the daily pattern of the SOGS data.

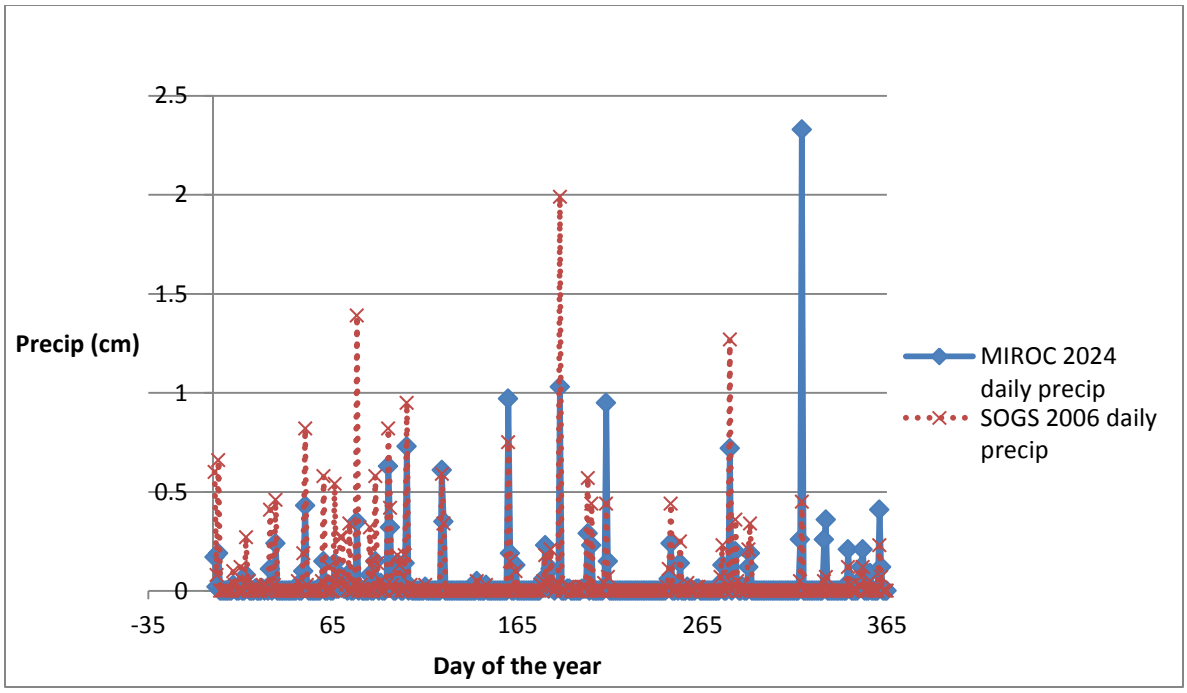

Figure 2-7 Temporally downscaled GCM versus SOGS precipitation data within one cell. The daily pattern was preserved but magnitudes were manipulated to match GCM monthly mean. Every month had a different scaling ratio.

2.2.4 Missing Variables

Four variables needed to run the Biome-BGC simulations were not given by the GCM and PRISM data sets: vapor pressure deficit (VPD), solar radiation (Srad), day length, and average daily temperature (T_{day}). To calculate vapor pressure deficit, solar radiation, and day length the MtClim algorithm was used driven by the downscaled daily data (Thornton 2000, Kimball 1997). T_{day} was calculated independently as:

$$0.45 * (T_{max} - \frac{T_{max} + T_{min}}{2}) + (\frac{T_{max} + T_{min}}{2})$$

T_{max} is the daily maximum temperature and T_{min} is the daily minimum temperature (Running and Coughlan 1988).

2.2.5 Spin-up problem

After running several test simulations throughout the entire study area, with standard parameter files describing shrubs, and C3 grasses and C4 grasses, it was apparent that shrubs were not growing where the land cover map indicated. C3 and C4 grasses, however, had spatial patterns matching expectations of their distribution. The majority of the problems arose in the southwestern United States. The original shrub runs offered by the spin-up model only covered 14% of the known extent of this rangeland type.

2.2.6 PRISM analysis

To model dryland areas, it is particularly important to understand water balance parameters to accurately represent how water limitation may affect NPP values. There is a strong relationship between soil moisture and plant water stress, meaning that as soil becomes drier, plants in this system experience exponential levels of stress, ultimately leading to mortality. These stress levels have exponential effects on productivity, at a certain point halting productivity all together (Porporato 2003a, Porporato 2003b). Rangeland environments are less productive then forests, especially in the southwest U.S., due very limited precipitation compared to forest ecosystems. When these areas are simulated by Biome-BGC, their production is so low that they approach mortality. I suspected that the PRISM historical precipitation data set may have been incorrect in these areas because water tends to be a limiting factor in rangelands. For this reason, analyses were conducted to quantify the precision and accuracy of PRISM versus weather station data across the southwestern United States. The seventy-eight stations that lie in this area from the U.S. Historical Climatology Network (HCN) (Karl 1990) were used for testing because this data set is readily accessible and easily analyzed. Yearly mean precipitation were calculated for both HCN and PRISM data at HCN locations from 1940-2001 (to match the length

of the PRISM data used). Then HCN data were subtracted from PRISM data to get an annual difference. The difference between HCN and PRISM data was then divided by the HCN data to get the annual percentage of error. An annual mean of these values was calculated over the 1940-2001 time period (Figure 2-8).

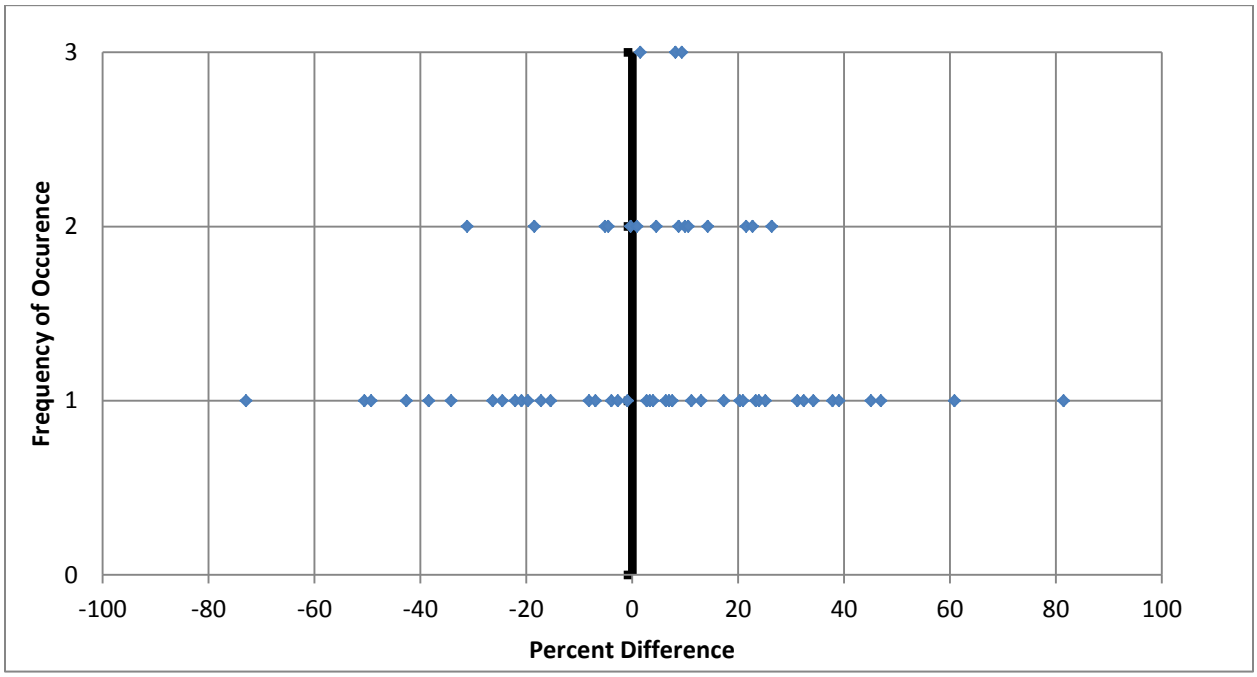

Figure 2-8 Number of occurrences of percent difference between PRISM and Weather Station precipitation data at 78 HCN stations from the southwestern United States. Negative values mean Prism had lower precipitation than reality. Positive values mean Prism had higher precipitation than reality.

The mean error between PRISM and weather station data was only 4.3 % with a standard deviation of 25.1. A mean error of 4.3% and a deviation of 25.1 shows a high level of accuracy but poor precision with respect to error as a percentage of mean annual rainfall. The difference between accuracy and precision is expected in areas that have plots with less than 1 mm of average daily precipitation. An error of 0.5 mm daily in PRISM data may be a significant difference in places with very little precipitation. Because the error in precision is centered on zero the only option to fix the problem of Biome-BGC not producing vegetation in areas where I know vegetation should exist was to modify the parameter files that describe the physiology of

the biome type. These results produced a high level of confidence in the data set. The scatter plot of the two maps values show a very linear 1 to 1 relationship (Figure 2-9).

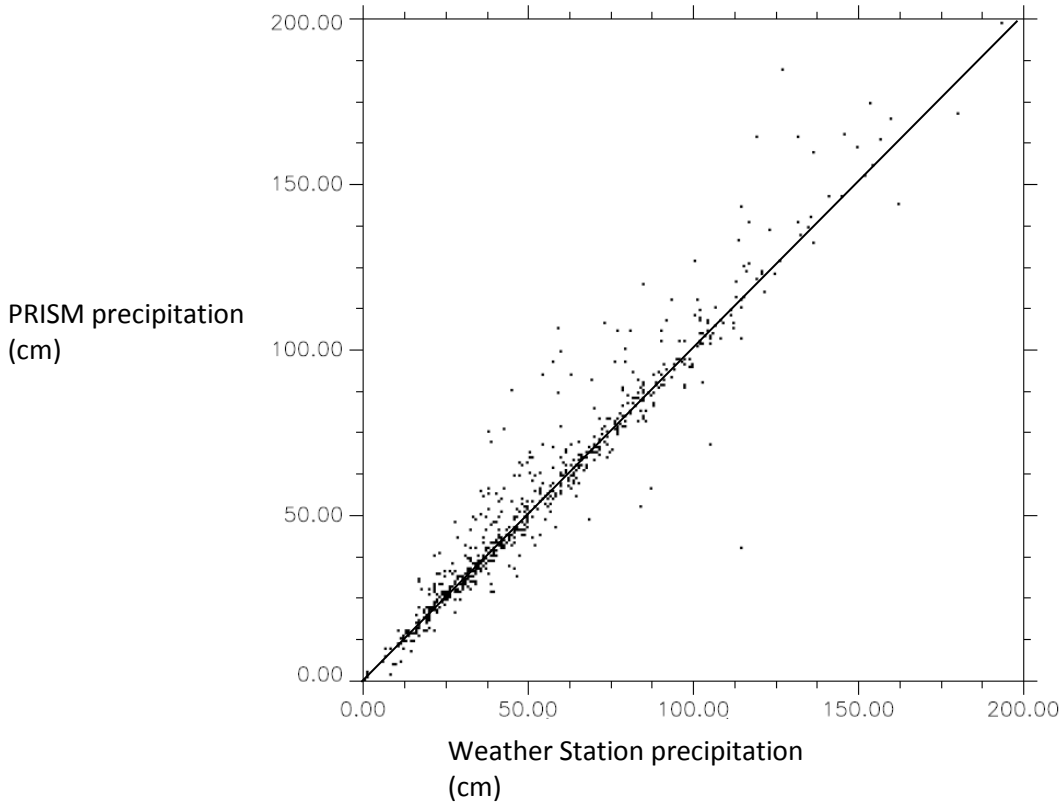

Figure 2-9 Sixty year mean annual precipitation of PRISM vs. HCN Weather Station observations from 1940 – 2000.

2.3 Parameterization and Model runs

2.3.1 Parameterization

Parameterization to describe shrub and C3 and C4 grass physiology was done to generalize these three land-cover types for the entire U.S. Because Biome-BGC does not allow for multiple cover types in a single simulation, simulations were performed for each of the three cover types as if the entire United States was composed entirely of each vegetation type. First the spin-up was performed using the PRISM climate data for each cover type. Once the spin-up was complete with calibrated parameters, projection runs were made using downscaled GCM data to drive the simulations. The simulations were run at daily intervals, running from 2001 to 2100 for each of the three Biome-types over the entire contiguous United States.

After these initial simulations were completed, pixels were filtered to show the extent of rangelands applicable to each land-cover type defined by Reeves and Mitchell (2010). To combine the three cover types into one cell, Landfire (Rollins 2009) data were used to determine the proportion of each cover type within the pixel, and the simulated values were then scaled accordingly to get a more accurate value of NPP. For example, a given cell contained 40% shrub land, 50% C3 grasses, and 10% C4 grasses, these percentages were multiplied by the simulated outputs to adjust the NPP approximation of the pixel value (Figure 2-10). The scaling method described made higher absolute values for each cover type because within each simulation there is no competition between species, each cover type is simulated individually. In some instances the percentages do not total to 100 percent. Not having a total of 100 percent cover in a cell indicates that there is some other vegetation type within the cell besides rangeland that is being ignored; these areas will be predicted to have less NPP than what would occur if the excluded cover type was also considered.

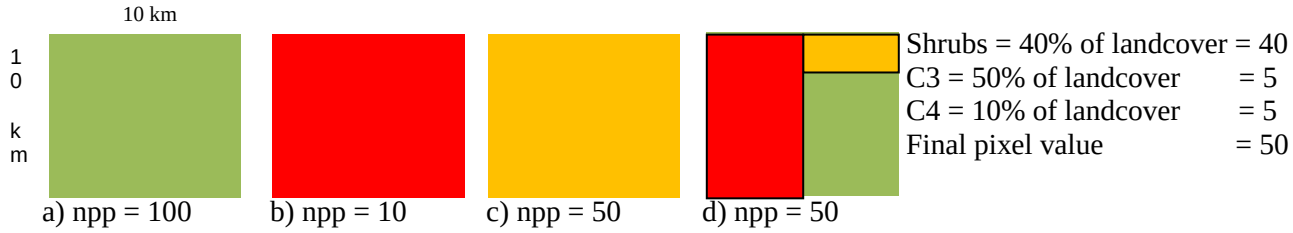

Figure 2-10 a) Simulation run with all shrubs. b) Simulation run with all C3 plants. c) Simulation run with all C4 plants. d) Pixel ajusted to total NPP value. The final NPP value for each cell was calculated by aggregating the NPP values of each cover type simulation scaled by its respective percent cover.

2.3.2 Development of new parameters

Because no shrubs were simulated after spin-up, further investigation was required to resolve the issue so that Biome-BGC would simulate shrubs in a larger portion than where they currently exist according to our land cover map. As described above, there is a high level of confidence in the climate data set so the problem had to lie in the parameterization of cover types. Using default parameters for grasses, their spatial patterns covered the extent of

grasslands as defined by the grassland map. Most studies that simulate shrubs use the White et al. (2000) parameters. However, many of the shrub parameters are assumed to be some percentage of another biome, most commonly evergreen needle leaf tree (Table A-7). The default shrub parameter file has been used in various publications (Mu 2008, Ma 2008), however, since southwestern U.S. ecosystems are barely productive (Svejcar 1997) in relation to other biomes that are traditionally simulated by Biome-BGC, the model had difficulty representing production over long periods of time. It took a few dry months to dramatically affect NPP and transpiration rates, and thus Biome-BGC results suggest that vegetation can no longer be grown in these locations. To modify the parameter files so that after spin ups Biome-BGC would more accurately populate a greater percentage of the known shrub-land area, a sensitivity analysis was done. The sensitivity analysis iteratively increased or decreased each parameter incrementally to see how that parameter affected the production of the biome type in these dry areas.

Biome-BGC was originally made to perform point simulations. Because this study covers such a large latitudinal gradient, the physiology of a typical shrub changes with the accompanying change in climate. The original parameters did work sufficiently for temperate shrub species found in more northerly latitudes. However, once the simulations moved into more southerly latitudes the parameters were unable to simulate the more xeric species of shrub found there. The inability of Biome-BGC to simulate shrubs in extremely hot and dry environments using the original parameters was because typically models are calibrated by choosing a location that has known LAI or NPP values and cover type and calibrate the model to match the values of this area. However, the technique described does not work over larger spatial extents as it creates parameters that are specialized for one particular area. Instead of focusing on values of LAI or NPP in one area, the focus became making the model cover a

correct spatial extent after spin-up. Though the outputs of the projections did not cover the intended spatial extent, they do cover all but the lowest producing areas. The approach taken in this study appears most appropriate for calibrating parameters over large spatial areas. Areas that could not be simulated correctly show extremes in climatic input values, very low percent cover, low precipitation, and very high VPD, maximum temperature, minimum temperature, and solar radiation values.

Tested cells were chosen at random that did not produce vegetation after spin-up in areas where there should be vegetation according to the land cover map. Then the sensitivity analysis was run on the shrub parameter file to detect which parameters would maintain vegetation growth at the end of spin-up. Once values were chosen that produced reasonable NPP values, a spatial run was performed to examine how well these parameters worked spatially. This produced vegetation in more desired cells, but typically left some cells unfilled. The process was then performed by testing cells that continued to be unfilled. After repeat testing and calibrating, results showed shrubs covering 84% of the known shrub land. The remaining 16% lie in very hot and dry regions that correspond relatively well with the areas that produce the lowest percentage of shrubs (Figure 2-11).

Once this satisfactory level of spatial coverage was reached, a literature review was done to examine the real world validity of the parameters that were calibrated (Table 2-12). All but current growth proportion for shrubs could be found in the literature. All values that were calibrated were very close, if not within, the range of the values found in the literature. Grass parameters were not modified as they covered a satisfactory spatial area.

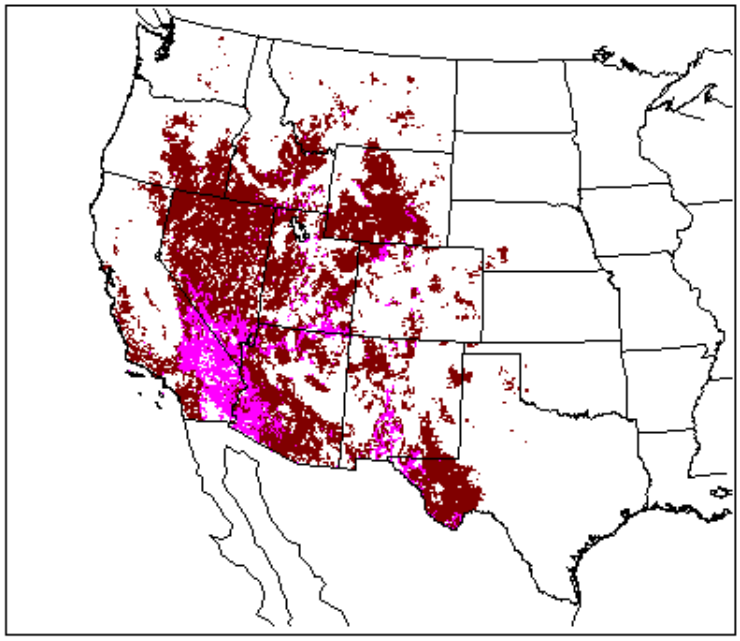

Figure 2-11 Map of cells that successfully simulated shrubs after spin-up using adjusted calibrated parameters for shrubs(red) and cells that did not indicate shrubs but where shrubs exists according to the land-cover map (Reeves 2009) (pink). Simulated cells = 15324 Total cells = 18217

Table 2-12 Shrub parameters that changed due to calibration. Listed are the orginal parameter values given by White et al. (2000), calibrated values, and the literature references that legitimize the values that were calibrated.

Parameter	Original (White et.al. 2000)	Calibrated	Verification Literature
annual leaf and fine root turnover fraction (and stem for perennial grass) (%biomass/yr)	0.32	0.16	Peek 2006
(ALLOCATION) new fine root C : new leaf C (ratio)	1.4	2.5	Mooney 1974
(ALLOCATION) new stem C : new leaf C (ratio)	0.22	0.145	Mooney 1974
(ALLOCATION) new live wood C : new total wood C (ratio)	1	0.5	Mooney 1974
C:N of leaves (ratio)	35	70	Schlesinger 1981
C:N of leaf litter (ratio)	75	150	Enriquez 1993
canopy average specific leaf area (m2/kgC)	12	4	Ackerly 2002
fraction of leaf N in Rubisco (fraction)	0.04	0.16	Ellsworth 2004
maximum stomatal conductance (m/s)	0.003	0.002	Woodward 1986

3 Results

3.1 Projection run

To examine the potential accuracy of the outputs of the projection run, the 10 year mean annual NPP from 2000 – 2010 was examined (Figure 3-1). The predicted values of NPP for this period ranged from 0 to 1100 g C/m^2/yr and averaged 135 g C/m^2/yr. Observed averages of global NPP for pasture land are approximately 350 g C/m^2/yr. (Field 2007). Contest-winning Iowa crops are roughly 2000 g C/m^2/yr. (Field 2007) which is essentially the upper-most limit of possible NPP for grasses in the western US.

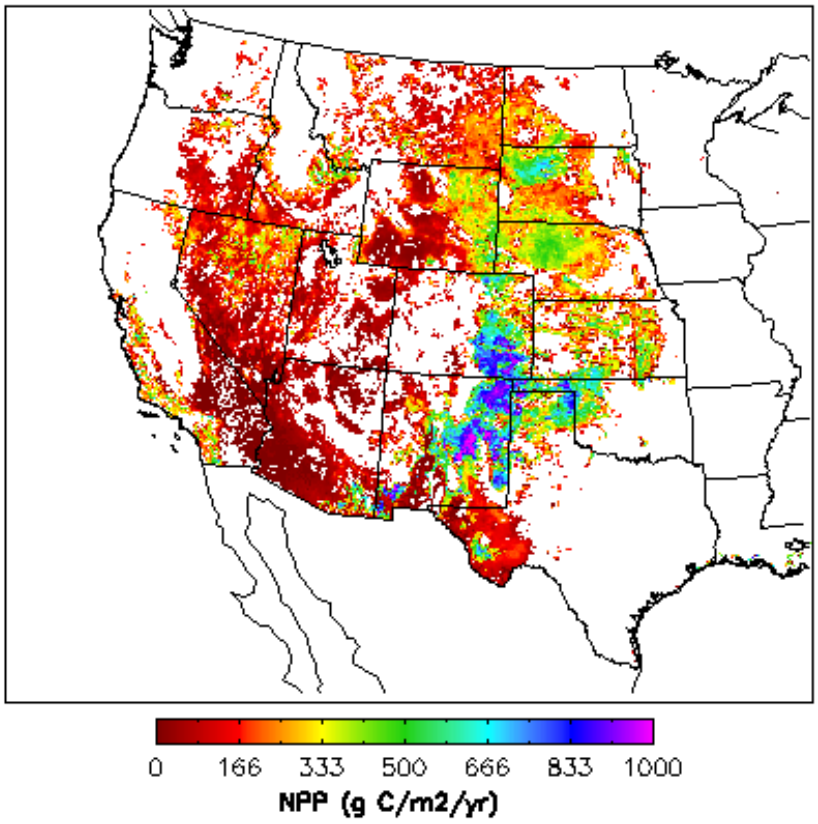

Figure 3-1 Simulated mean annual NPP of United States rangelands from 2000-2010 (g C/m^2/year).

The areas with the lowest predicted productivity tended to be in the shrub lands. The highest NPP values for shrub lands were located in Northern Nevada, southern Oregon and Idaho

of the Great Basin, and along the southern Californian coast, whereas the highest predicted NPP values for grasslands are in the Northern Texas, Oklahoma, Kansas, Colorado and New Mexico regions of the Great Plains. The lowest NPP(s) for shrub lands are found in the Death Valley, Sonoran and Mojave basin regions. The lowest predicted NPP values for grasslands are in the northern latitudes and a small section in New Mexico.

3.2 Agreement with MODIS:

Though MODIS is a model itself MODIS is widely used and validated across many land cover types and is used in many studies globally. Even though MODIS data is not observed field data it can give a good idea of realistic ranges of NPP values and the corresponding spatial pattern. The numbers shown in the Table3-2 show the Biome-BGC simulated data as compared to MODIS data values.

Table3-2 Statistics of Biome-BGC (predicted) vs. MODIS (observed)

Overall General Stats:	Observed	Predicted	Delta
Mean	227.76	135.39	-92.38
min	0	0	-1349.3
max	1483.93	663.15	502.40
count	30544	30544	30544
Model Performance Stats:			
MBE	-92.38		
MAE	130.05		
RMSE	172.66		
Ind. Agreement, d	0.49		

Through large swaths of land stretching from eastern Oregon to eastern Wyoming and from southwestern Montana to the Mexican border, Biome-BGC matched MODIS NPP patterns. In the area around the confluence of New Mexico, Texas, Oklahoma, Colorado, and Kansas, Biome-BGC consistently overestimated NPP, while on the Californian coast and through the

middle of Montana and the Dakotas, Biome-BGC underestimated NPP compared to MODIS(Figure 3-3).

MODIS NPP differences with Biome-BGC taper off at approximately positive and negative 500. The histogram in Figure 3-4 of the error shows that accuracy of Biome-BGC compared to MODIS. Sixty eight percent of difference values lie within one standard deviation of 0. The peak of values close to 0 and the majority of cells lying within 1 standard deviation show a high level of both accuracy and precision of Biome-BGC when compared to MODIS. The high accuracy and precision of the difference along with a difference map shows that Biome-BGC produced values that were in a realistic range and a desired spatial pattern.

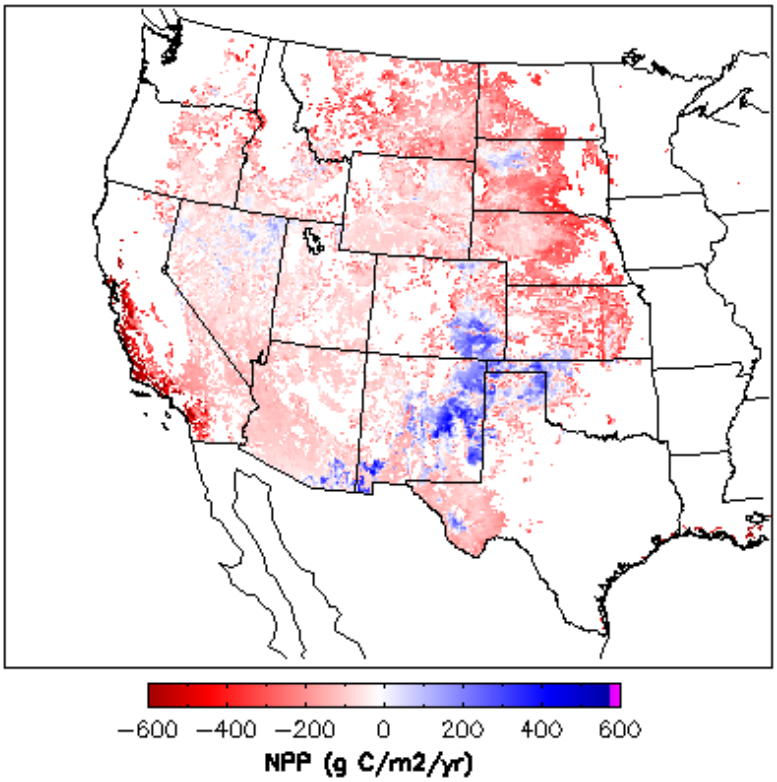

Figure 3-3 Biome-BGC minus MODIS. Biome-BGC under-predicts NPP compared to MODIS data in the vast majority of cells.

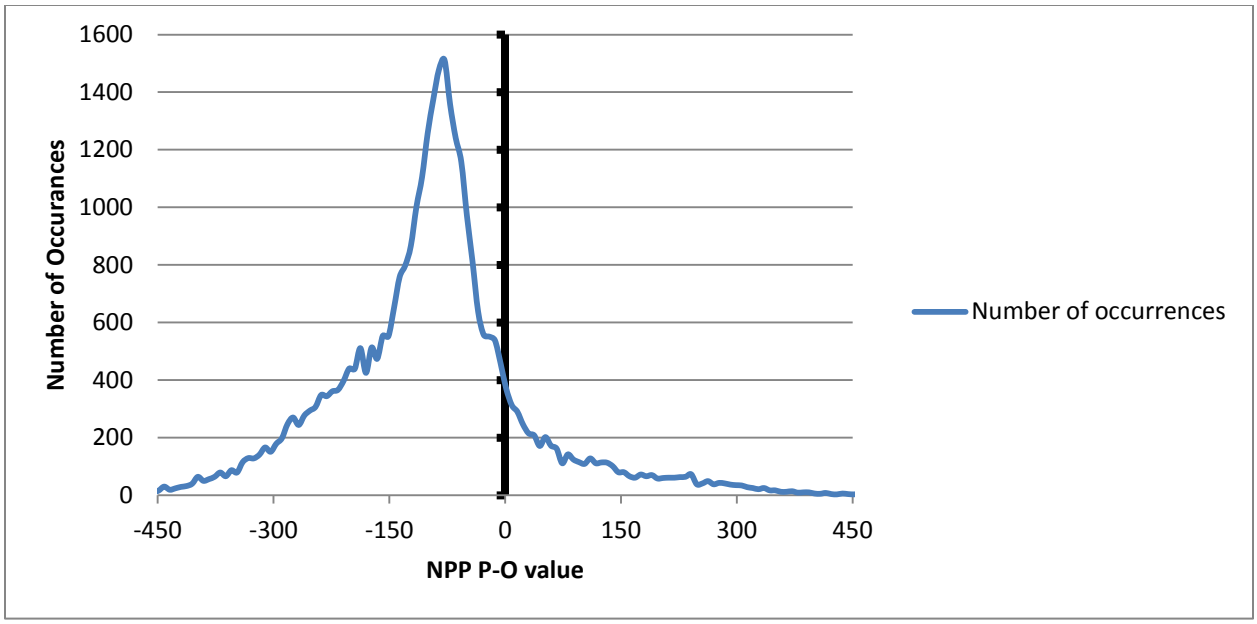

Figure 3-4 Biome-BGC (predicted) minus MODIS (observed) average annual NPP for United States rangelands from 2000-2009.

3.3 Trends

The magnitude of the mean annual predicted NPP over the 100 year time period was calculated to show the areas with the overall highest and lowest productivity (Figure 3-5). The Great Plains east of the Rocky Mountains have the highest overall productivity followed by the Great Basin south of Idaho. The areas with the lowest productivity are in the southwestern portion of the United States in the Mojave and Sonoran basins. Biome-BGC was unable to simulate vegetation in most of the Mojave basin due to the extreme paucity in annual precipitation. The Mojave basin experiences close to an average of 0 mm of precipitation daily and using the parameter files for shrubs and grasses this area experiences a water stress index of 365 meaning that growth is restricted by precipitation every day of the year. The water stress index (WSI) equals the soil moisture growing season index multiplier multiplied by the vapor pressure deficit growing season index multiplier. A WSI of 0 indicates that growth is never restricted by moisture and a value of 365 indicates that every day growth is completely restricted by moisture.

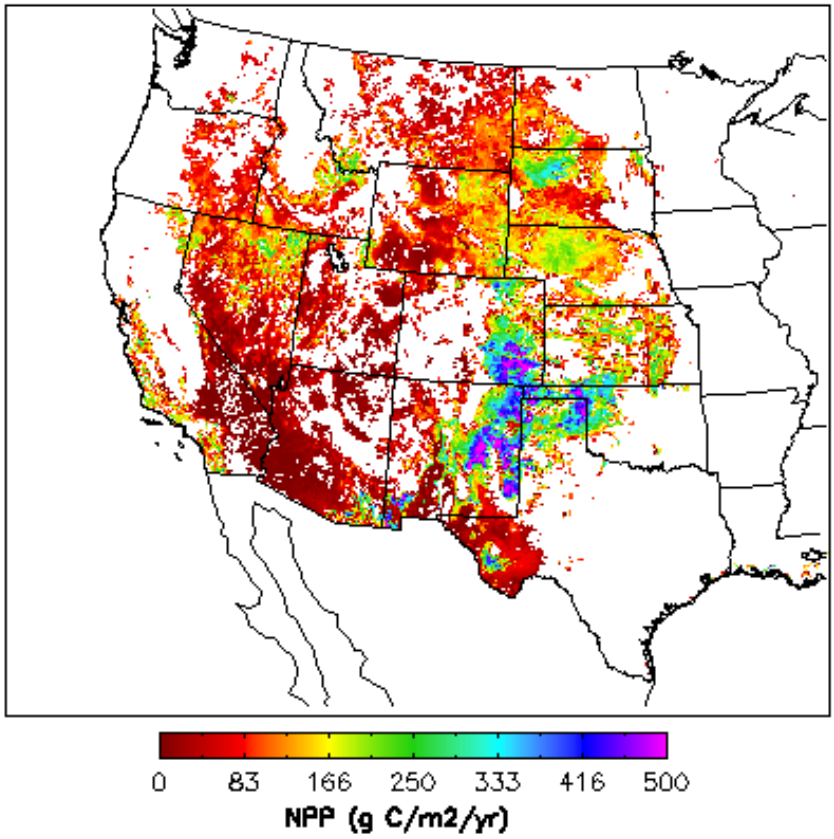

Figure 3-5 Mean annual NPP (gC/m2/yr) of United States rangelands from 2001-2100 range 0 – 609 mean = 107

Overall trends show that mean annual NPP for all rangelands will have an increase of 0.24 g C/m^2/yr (Figure 3-6). To spatially understand how NPP trends are projected to change over the next 100 years, every cell had a linear regression model calculated from the simulation's NPP values of that cell through time (Figure 3-7). Fifty-five percent of cells have no statistically significant change. The spatial distribution of the trends shows three distinct zones of trends. The southwestern part of the United States, including the Mojave and Sonoran basins, shows a marked decline in NPP over the next 100 years. Those states that lie north of Colorado show little change throughout the region with the exception of two pockets of substantial increase in the Idaho-Montana region of the Great basin and in the Dakotas. The zone that shows the greatest increase lies in the New Mexico, Texas, Oklahoma, Colorado, and Kansas portions of the Great Plains.

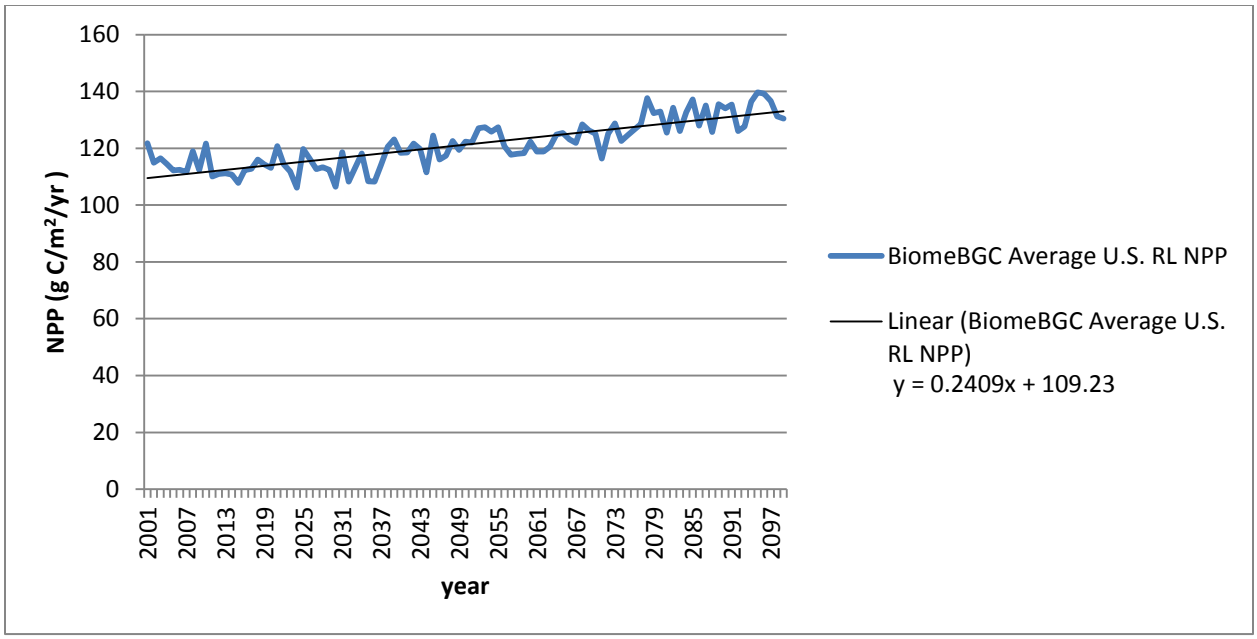

Figure 3-6 Overall 10km US Rangeland projected mean annual NPP trends from 2001-2100.

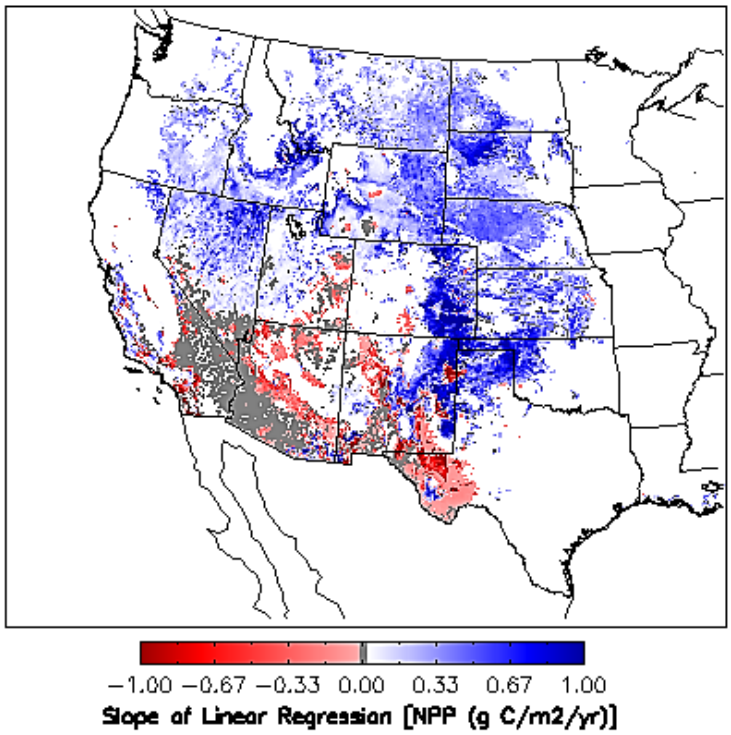

Figure 3-7 Slope of linear regression for U.S. projected mean annual NPP projection from 2001-2100.

4 Discussion

The first ten years of our projected simulation gives an idea of the spatial distribution of rangeland NPP and how well model can simulate the current distribution of this cover type. As stated earlier, these values are meant as a maximum potential NPP of the rangeland portion of each cell that these lands can sustain and do not necessarily represent real world values that will be realized. Areas with the most favorable climate conditions produced by the GCM for NPP have higher NPP in the simulation. Conversely the areas with the lowest NPP were in areas with drier climatology and low nitrogen deposition. There is also higher NPP in areas with greater N deposition, meaning that areas east of the Rocky Mountains typically have higher NPP.

4.1 Trends

Trends show that over the next 100 years the United States could see an increase of overall NPP from its rangelands by approximately 0.24 g $C/m^2/yr$. The year to year variation ranges from 0 to 15 g $C/m^2/yr$ due to the natural yearly variability in climatic factors such as temperature and precipitation built into the GCM data set. A graph showing a 10 year moving average of projected mean annual NPP plotted against a selection of the projected input variables used in the Biome-BGC show that NPP correlates more strongly with different variables at different points in time (Figure 4-1). NPP tends to stay steady or slightly decrease until about 2036 then increase again. The pattern of projected NPP appears to match mean annual precipitation until about the year 2055 when precipitation plummets but NPP only slightly decrease while maintaining an upward trajectory of NPP. After year 2055 it can be surmised that NPP starts to follow temperature and does so until the end of our projections. NPP showed little to no correlation with nitrogen deposition which was interesting because I originally hypothesized that NPP would be largely influenced by nitrogen deposition. The lack of

correlation between NPP and nitrogen deposition indicates that these lands might not be as nitrogen limited as originally thought. The lack of response to nitrogen deposition could be real or the result of inaccurate parameterization of the cover types does not accurately reflecting how this vegetation uses nitrogen or that Biome-BGC does not modulate growth response to nitrogen effectively.

One reason for the reverse in downward trend in NPP is the increase in minimum temperature. A steep increase in minimum temperature may have allowed for a longer growing season without having a dramatic increase in evapotranspiration.

Figure 4-4 may indicate that the benefit in a lengthened growing season out paces the disadvantages of increasing evapotranspiration because the correlation map shows that northern latitudes' NPP is most correlated to temperature. The histogram of correlation (Figure 4-5) shows that a large portion of the study area is primarily correlated with minimum temperature supports the theory of the effect of growing season having a greater effect on NPP then evapotranspiration. Also, if one compares the areas that are highly correlated with minimum temperature with the maps of NPP trends I see that these areas are some of the fastest increasing locations. In the histogram it is evident that minimum temperature rises at nearly the same rate as CO_2 concentration. The correlation between minimum temperatures and CO_2 concentration is also shown in the correlation map where areas that are highly correlated with minimum temperature contain dispersed patches of areas that are highly correlated with CO_2 concentration.

Once NPP begins to increase nationally around the year 2036, NPP begins to follow both maximum temperature and VPD. Maximum temperature and VPD have almost identical patterns throughout the years. This makes sense since maximum temperature often increases evaporation, lower relative humidity and will increase vapor pressure deficit in areas that are already water limited as are rangelands. The reason that NPP is not decreasing across the entire

study area is that the areas that are seeing the highest increase in VPD are areas that have the lowest NPP. These areas will not highly influence the overall trend of NPP across the entire study area.

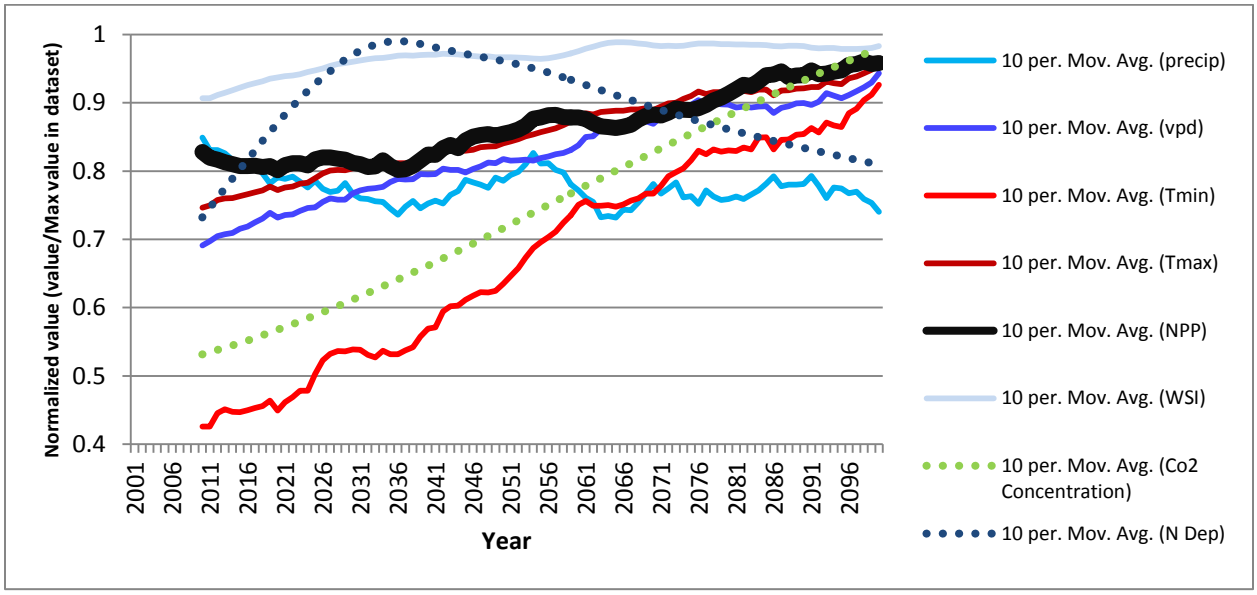

Figure 4-1 Normalized 10 year moving avg. of climatic inputs and average annual NPP of U.S. rangelands from 2001-2100

When one looks at the difference between the first 10 years of our simulation and thirty year averages there is a trend toward an increase in potential NPP. Three thirty-year averages were calculated: the 2020s (2010 – 2039), 2040s (2030 – 2059), and 2080s (2070 – 2099) (Figure 4-2). There is a clear dominance of cells that have no change. There are 4155 cells with average occurrence of values of 0. However, of those cells that do change, there is a tendency for cells that have lower NPP than the 10 year baseline to increase in production as shown by a decrease in the number of cells that are negative. As time progresses the greatest values of potential NPP in rangelands become even more productive and that the number of cells with higher NPP than the base increase throughout time.

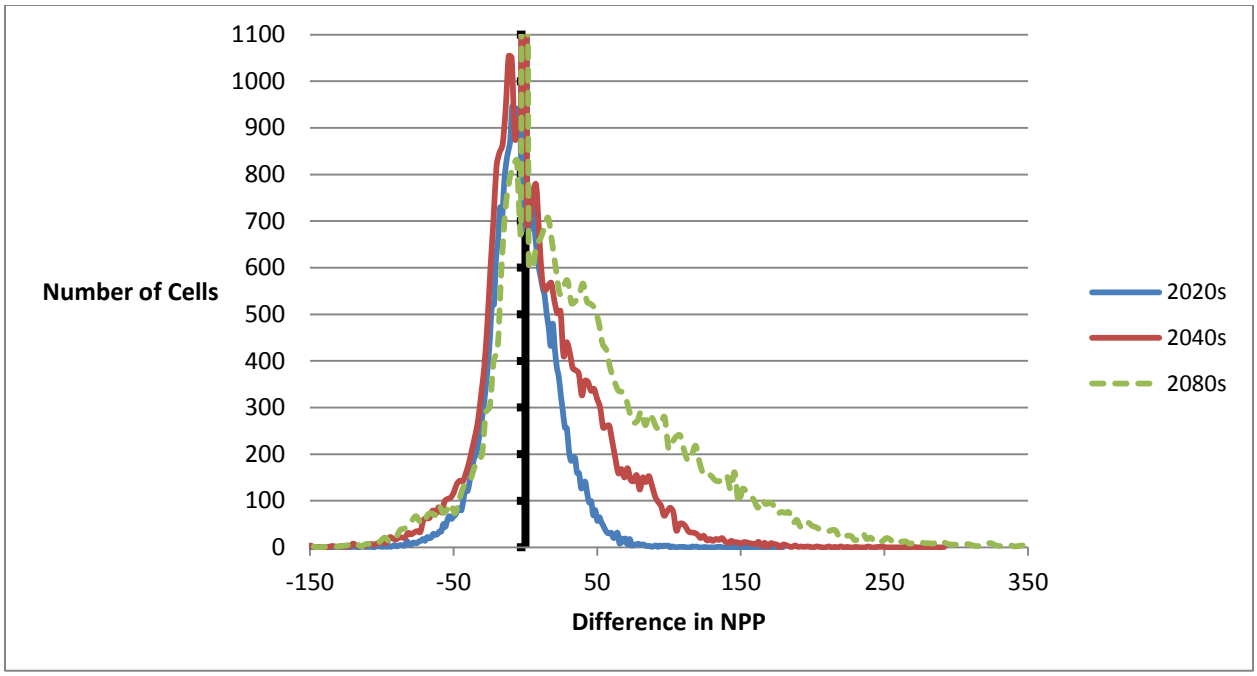

Figure 4-2 Thirty year mean minus Baseline (2001-2010). The average occurrence of cells with 0 differences was 4155. 2020s (2010 – 2039), 2040s (2030 – 2059), and 2080s (2070 – 2099)

The spatial occurrences of the slope of individual cells' linear regressions show that the majority of cells, 4163 cells, have little to no gain (Figure 4-3). Of the cells that have noticeable change there is a clear peak of the number of cells with a slope of 0.18. The majority of cells having a positive trend indicate that there may be an increase in projected NPP over the next 100 years, but 55% of cells have no statistically significant change in projected NPP.

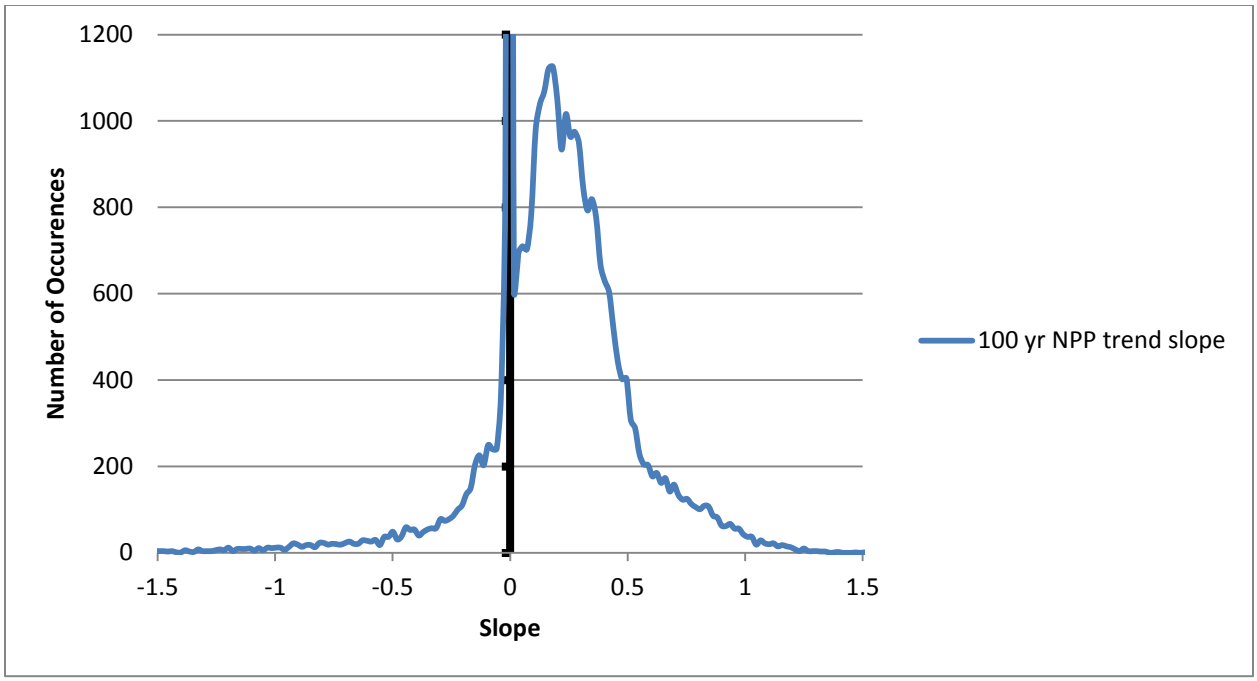

Figure 4-3 Spatial occurrences of Linear Regression Slope values of cells in U.S. rangelands calculated over 2001-2100.

The spatial distribution of trends shows that the majority of the area outside of the southwest has a trend of increasing NPP. The zone with the greatest increase is just north of Texas. The increase is primarily due to the increase of production in C4 grasses. The Great Plains north of Texas shows a large decrease in shrubs and a slight decrease in C3 grasses but a large increase in C4 grasses due to the higher tolerance of the C4 photosynthetic pathway to maximum temperatures which are increasing in this region. The other areas that show increases in NPP, primarily in the Great Basin, show a mix of increases from C4, C3 and shrub's NPP. The areas that show a general decrease tend to see higher decreases in shrubs than either of the grasses. The reason that shrubs decrease more than grasses could be due to the higher maintenance cost in shrubs. Shrubs have to withstand the winter as perennials and have higher biomass than grasses leading to higher maintenance respiration and perhaps greater stress over time.

4.2 Correlation

Using the map of highest correlating input variables allows insight into why there is spatial variation (Figure 4-4). The climatic reasons behind the increases and decreases spatially vary from region to region. In the already hot and dry southwestern part of the United States precipitation in all of its facets plays the greatest role in limiting projected NPP. The climatology that was used to produce the projections shows a decrease in precipitation in the southwest throughout the next 100 years. The southwest contains the vast majority of area that has decreasing NPP. The southwest is also the area with the least precipitation. It is not surprising that in an area already so limited by water one sees large decreases in this area's relative potential NPP with decreasing annual precipitation.

The rangeland in the Great Plains east of the Rocky Mountains shows the greatest increase in relative potential NPP. The increase in NPP is due almost entirely to C4 grasses. Both shrubs and C3 grasses show overall decreases in this area, specifically in the southern portion of the Rocky Mountain Great Plains. The decrease in shrubs and C3 grasses is primarily due to the decrease in precipitation and the increase in VPD that doesn't affect C4 grasses to the same extent (Kawamitsu 1993). The correlation map shows that NPP in the Rocky Mountain Great Plains area is most correlated with minimum temperature and CO_2 concentration. Minimum temperature is shown to increase which can lengthen the growing season and increase NPP if daily production rates remains the same. The climatology also shows that the WSI in this region will slightly change. The minimal changes in climatology give us reason to believe that daily NPP in the Rocky Mountain Great Plains area might increase or remain the same. Increases in VPD in all areas are worth noting. However, the Rocky Mountain Great Plains area has a low VPD in the early decades compared with other rangelands at the same latitude. This can help the region cope with an increasing VPD because the region is starting off lower than average.

The northwest and parts of Nevada in the Great Basin show a moderate increase in NPP. The Nevada portion of the Great Basin however, is largely controlled by a slight decrease in solar radiation. The way in which we calculated solar radiation is a function of the difference in minimum and maximum temperature. The Nevada portion of the Great Basin will see higher than average increases in minimum temperatures and lower than average increases in maximum temperature. The discrepancy between rates of increase between minimum and maximum temperature results in a decreasing difference between the two. A decreasing difference in minimum and maximum temperatures through time will result in continuously decreasing solar radiation. Therefore, the correlation with solar radiation actually indicates a correlation with the difference between minimum and maximum temperatures. Solar radiation will slightly decrease according to our calculations in the Nevada portion of the Great Basin over the next 100 years. The decrease in solar radiation, and the decrease in temperature difference that drives solar radiation, corresponds with the slight increases in NPP of the region. A decrease in the difference between minimum and maximum temperatures indicates increasing humidity and, because both minimum and maximum temperatures are increasing, also a lengthening in growing season length that out paces losses due to increased respiration. Both an increase in humidity and an increase in growing season length are conducive to increases in NPP.

The area that sees the greatest decrease is in the Southwestern United States in the Sonoran and Mojave basin regions. The Southwestern United States has the lowest NPP in absolute terms. The low NPP in the Southwestern United States means that the decreases in the area do not largely affect the overall trends in rangeland NPP. Precipitation and VPD are the major contributing factors in NPP in this area both of which are on a drying trend. The driest areas in the nation are found in the Southwestern United States so any change in moisture will greatly affect the NPP.

Most interesting to note is that Biome-BGC did create three distinct regions within the nation's rangelands. The first region is the south western portion of the United States. The south western portion of the United States has decreasing NPP and is largely influenced by precipitation and VPD. The second region is the area around the Great Basin that sees slight increases in NPP and is largely influenced by solar radiation. The third region is the Great Plains and is largely influenced by temperature and CO_2 concentration.

The climatic variables that most affect rangeland NPP is minimum temperature (Figure 4-5). The large influence minimum temperature has on NPP is primarily seen in the Great Plains. The correlation between minimum temperatures and NPP indicates that with an increase in growing season length due to the rising minimum temperatures rangelands will see large increases in NPP. The second highest influencing climatic variable is solar radiation that greatly influences the Great Basin throughout the west. NPP is negatively correlated with solar radiation here and indicates that with higher precipitation and lower than average increases in maximum temperature will produce little to no change in NPP. The third highest correlating variable is the sum of all of the moisture and precipitation variables. Moisture and precipitation variables primarily affect the south west. The south west is showing lower moisture and thus lower NPP. Other variables to make notice of are CO_2 concentration and maximum temperature. These variables influence a large amount of area that mostly lie on opposite ends of the Great Plains with CO_2 affecting a large southern portion and maximum temperature affecting the northern. As discussed earlier, CO_2 is highly correlated with minimum temperature and this variable highly influences the growing season length indicating this area is still being influenced by growing season length even though CO_2 concentration is the greatest correlating variable. A growing season limitation due to snow cover instead of strictly phenological constraints in the northern portion of the Great Plains is caused by increases in maximum temperature decreasing

the duration of snow cover. The correlation with maximum temperature can also indicate that these areas are limited by temperature during the photosynthetically active time of day which can be consistent with the northern latitudes of the United States.

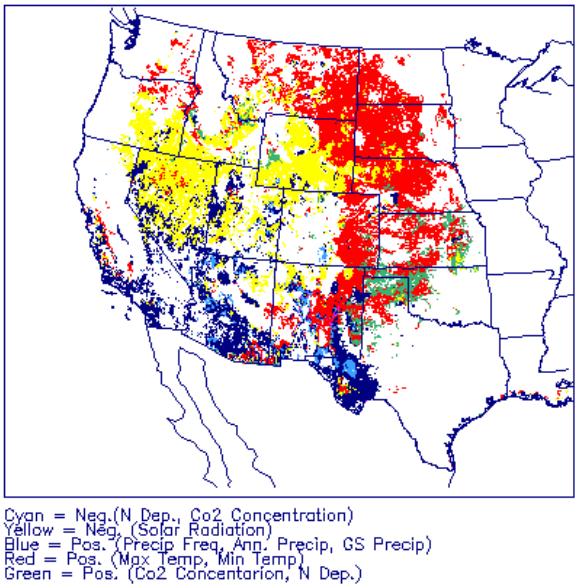

Figure 4-4 Spearman Correlation of U.S. rangeland NPP vs input variables from 2001-2100. Cyan and yellow have negative correlations while blue, red and green indicate positive correlations. These colors do not indicate whether NPP was increasing or decreasing.

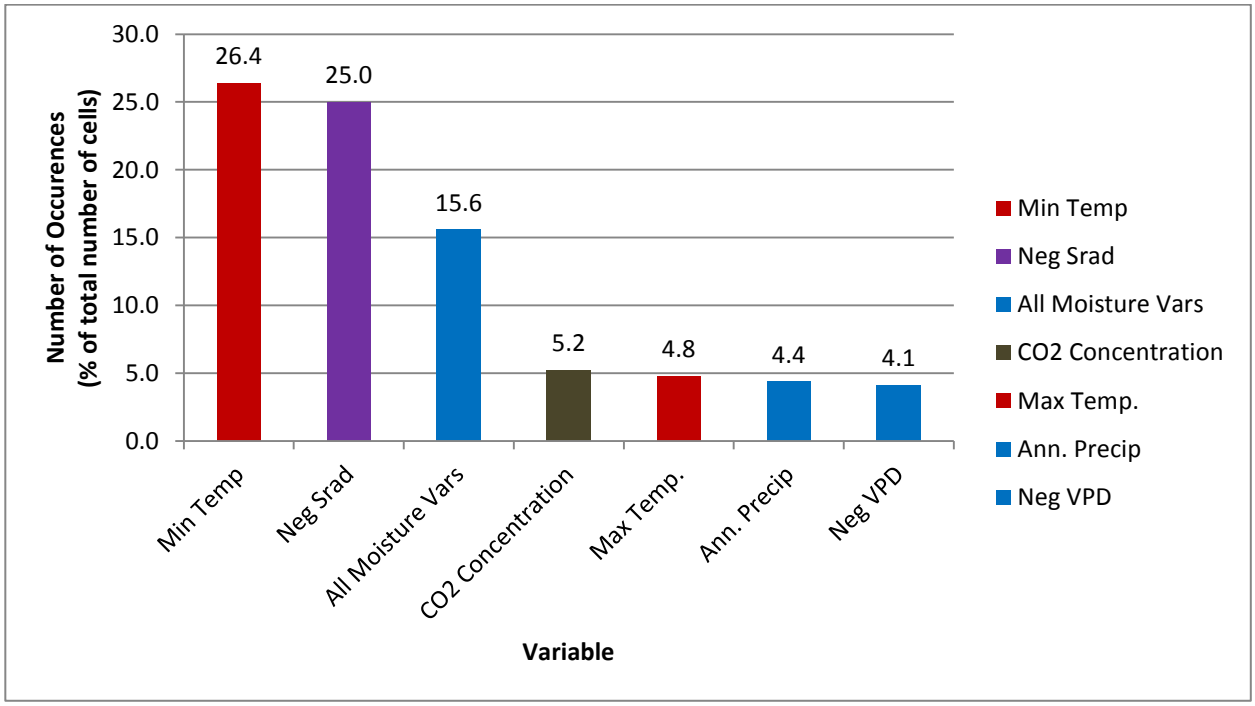

Figure 4-5 Number of occurrences of spearman correlations of NPP vs. input variables as a percentage of total cells for U.S. rangeland from 2001-2100. Only variables that covered 4% or more of the cells are shown.

5 Conclusions

In the face of climate change, it is crucial to study and understand how our landscapes may change, whether change comes in the form of rising sea levels, melting glaciers, or insect outbreaks. Though lower in productivity than forests, rangeland ecosystems provide society with necessary functions including watershed management, grazing land, habitat for native species and carbon sequestration. To project how climate change may impact vital rangeland habitats of the U.S., understanding future vegetative productivity is important to ensure that society is prepared for the shifts in production that may occur.

This study shows that potential NPP of the majority of U.S. rangelands is projected to increase slightly. The increasing trend in potential NPP is not distributed equally throughout the landscape. NPP for shrub lands of the southwest is projected to significantly decline, and the productivity of grasslands in the Great Plains east of the Rocky Mountains is projected to increase considerably. The reason for these spatial differences is due to climatological factors that will be affected by climate change throughout the United States in the rest of the century.

It is important to understand where the nation's rangelands may sustain pressure from human appropriation of NPP and which areas may be unable to sustain the same level of use they do today. As demand for ecosystem services rises with the increase in human population and increased development activities, understanding those regions in danger of losing vegetative production and the regions that may yield higher productivity due to climate change is important for future land planning and management.

Furthermore, not all rangelands are made equal. Large swaths of grasslands may become more productive, yet they cannot fulfill the role that shrub lands play for various animal species both wild and domesticated. Likewise, if range lands east of the Rockies become more productive over time, this does nothing for the inhabitants of the southwest where their rangelands may become increasingly less productive.

Further research in this area could incorporate more accurate vegetation behavior. For example, one could create different C3, C4, and shrubs parameterization files for the various eco-regions and latitudes. Further calibration of the cover type parameters could be performed because of the difficulty in finding some parameters in the literature.

It is also clear that Biome-BGC has a difficult time simulating dryland ecoregions. Further model development is needed to be able to accurately simulate these biomes. Improvements in Biome-BGC could come in the form of specific algorithms that target xeric systems more specifically grasses and shrubs. Models have a difficult time simulating growing season. How Biome-BGC models growing season length is also an area that requires further investigation because of the dependency the results have on growing season length.

There are also numerous sources of climate data and several ways that this data can be downscaled. Using different climate data sets would give us more confidence in the results by being reproduced and corroborated using different GCM's and CO_2 emissions scenarios. Given that the IPCC is about to release AR 5 GCM data sets it would be interesting to determine how much of a difference these new data sets would make on our results.

6 References

Ackerly, D. D., Knight, C. A., Weiss, S. B., Barton, K., Starmer, K. P. 2002. Leaf Size, Specific Leaf Area and Microhabitat Distribution of Chaparral Woody Plants: Contrasting Patterns in Species Level and Community Level Analyses. Oecologia, 130: 449-457

Baker, B. B., J. D. Hanson, R. M. Bourdon, and J. B. Eckert. 1993. "The Potential Effects of Climate Change on Ecosystem Processes and Cattle Production on U.S. Rangelands." Climatic Change. 23:97-117

Batjes, N. H. 1998. Migration of atmospheric CO2 concentrations by increased carbon sequestration in the soil. Biology and Fertility of Soils 27:230-235

Briske, D.D., S.D. Fuhendorf, F.E. Smeins. 2005. State-and-transition models, thresholds, and rangeland health: a synthesis of ecological concepts and perspectives. Rangeland Ecology and Management 58:1-1

Brown, J.R., Bestelmeyer, B., Havstad, K. 2008. Rangeland ecology and management in a changing world. Multifunctional Grasslands in a Changing World Volume. 1: 41-45

Brown, J.R., Thorpe, J. (2008). Climate change and rangelands: responding rationally to uncertainty. Rangelands 30,3–6. Cambridge University Press

Buis GM, Blair JM, Burkepile DE, Burns CE, Chamberlain AJ, Chapman PL, Collins SL, Fynn RWS, Govender N, Kirkman KP, Smith MD, Knapp AK. 2009. Controls of aboveground net primary production in mesic savanna grasslands: an inter-hemisphere comparison. Ecosystems 12:982–9

Climate Impacts Group 2009. *The Washington Climate Change Impacts Assessment*. M. McGuire Elsner, J. Littell, and L. Whitely Binder (eds). Center for Science in the Earth System, Joint Institute for the Study of the Atmosphere and Oceans, University of Washington, Seattle, Washington.

Conway, T.J., P.P., Waterman, L.S., Thoning, K. W., Kinis, D.R., Masarie, K.A. and Zhang, N. 1994. Evidence for interannual variability of the carbon cycle from the National Oceanic and Atmospheric Administration/Climate Monitoring and Diagnostics Laboratory global air sampling network, J. Geophys. Res. 99: 22831-22856

Costanza, R., d'Arge, R., Groot, R., Farber, S., Grasso, M., Hannon, B., Limburg, K., Naeem, S., O'Neill, R.V., Paruelo, J., Raskin, R.G., Sutton, P., van den Belt, M., 1997. The value of the world's ecosystem services and natural capital. Nature 387: 253–26

Costanza, R., Fisher, B., Mulder, K., Liu, S., Christopher, T., 2007. Biodiversity and ecosystem services: a multi-scale empirical study of the relationship between species richness and net primary production. Ecological Economics 61: 478–491

Coughenour M.B., Chen D.X. 1997. Assessment of grassland ecosystem responses to atmospheric change using linked plantsoil process models. Ecological Applications 7: 802–827

Coulson, David P., Joyce, Linda A., Price, David T., McKenney, Daniel W. 2010. Climate Scenarios for the conterminous United States at the 5 arc minute grid spatial scale using SRES scenario B2 and PRISM climatology. Fort Collins, CO: U.S. Department of Agriculture, Forest Service, Rocky Mountain Research Station. Available: http://www.fs.fed.us/rm/data_archive/dataaccess/US_ClimateScenarios_grid_B2_PRISM.shtml [2010, August 2].

Daly C, Taylor GH, Gibson WP, Parzybok TW, Johnson GL, Pasteris P (2001) High-quality spatial climate data sets for the United States and beyond. Trans Am Soc Agric Eng 43:1957–1962

Di Vittorio, A., V., Anderson, R. S., White, J. D., Miller, N. L., Running, S. W. 2010. Development and optimization of an Agro-BGC ecosystem model for C4 perennial grasses. Ecological Modeling, 17: 2038-2053

Dukes JS, Chiariello NR, Cleland EE, Moore LA, Shaw MR, et al. 2005. Responses of grassland production to single and multiple global environmental changes. PLoS Biol. 3:1829–37

Duvick, D.N. and Cassman, K.G. 1999. Post-Green Revolution trends in yield potential of temperate maize in the North-Central United States. Crop Sci. 39: 1622–1630

Ellsworth, D., S., Reich, P. B., Naumburg, E. S., Kochs, G. W., Kubiske, M. E., Smith, S. D. 2004. Photosynthesis, carboxylation and leaf nitrogen responses of 16 species to elevated CO_2 across four free-air CO_2 enrichment experiments in forest, grassland and desert. Global Change Biology, 10: 2121-2138

Enriquez, S., Duarte, C. M., Sand-Jensen, K. 1993. Patterns in Decomposition Rates among Photosynthetic Organisms: The importance of Detritus C:N:P content. Oecologia, 94: 457-471

Field, C. B., Campbell, J. E, Lobell, D. B. 2007 Biomass energy: the scale of potential resource. Trends in ecology and evolution 23: 65-72.

Field, C. B., Jackson, R.B. & Mooney, H. A. (1995). Stomatal responses to increased CO_2: implications from the plant to the global scale. Plant, Cell and Environment 18: 1214–1225.
Fox, W., McCollum, D., Mitchell, J., Swanson, L., Kreuter, U., Tanaka, J., Evans, G., Heintz, H., Breckenridge, R., Geissler, P., 2009. An Integrated Social, Economic, and Ecologic Conceptual (ISEEC) framework for considering rangeland sustainability. Society and Natural Resources 22 (7), 593–60
Fredeen, A. L., Randerson, J. T., Holbrook, N.M. & Feild, C. B. (1997). Elevated atmospheric CO_2 increases water availability in a water-limited grassland ecosystem. Journal of the American Water Resources Association 33: 1033–1039.
Golinkoff, J. (2010). Biome BGC version 4.2 Theoretical Framework of Biome-BGC. In progress.
Gordon, W. S., Jackson, R. B. 2000. Nutrient Concentrations in Fine Roots. Ecology, 81: 275-280
Grunzweif, J.M. & Korner, C. (2001). Growth, water and nitrogen relations in grassland model ecosystems of the A framework to interpret variability in CO_2 responses 11 semi-arid Negev of Israel exposed to elevated CO_2. Oecologia 128: 251–262.
Hansen, J., R. Ruedy, M. Sato, M. Imhoff, W. Lawrence, D. Easterling, T. Peterson, and T. Karl. 2001. A closer look at United States and global surface temperature change, J. Geophys. Res., 106: 23,947–23,963.
Havstad, K., D. Peters, B. Allen-Diaz, J. Bartolome, B. Bestelmeyer, D. Briske, J. Brown, M. Brunson, J. Herrick, L. Huntsinger, P. Johnson, L. Joyce, R. Pieper, T. Svejcar, and J. Yao. 2009. The Western United States Rangelands: A Major Resource. pp.75-93. In: W.F. Wedin, and S.L. Fales [eds.]. Grasslands: Quietness and Strength for a New American Agriculture. Soil Science Society of America: Madison, WI, USA.
Holland, E. A., Braswell, B. H., Sulzman, J. & Lamarque, J. F. 2005. Nitrogen deposition onto the United States and Western Europe: synthesis of observations and models. Ecol. Appl. 15: 38–57
Houghton, J. T. et al. Climate change 2001: the Scientific Basis. Contributions of Working Group I to the Third Assessment Report of the Intergovernmental Panel on Climate Change (Cambridge Univ. Press, 2001).
Houlton, B.Z., and C.B. Field. 2010. Nutrient limitations of carbon uptake: From leaves to landscapes in a California rangeland ecosystem. Rangeland Ecol. Manag. 63:120-127.
Hunt, H. W., E. R. Ingham, D. C. Coleman, E. T. Elliott, and C. P. P. Reid. 1988. Nitrogen limitation of production and decomposition in prairie, mountain meadow, and pine forest. Ecology 69:1009-1016.
IPCC. (2001). Climate Change 2001: The Third IPCC Assessment Report: Intergovernmental Panel on Climate Change. e [Houghton, J.T., Y. Ding, D.J. Griggs, M. Noguer, P.J. van der Linden, X. Dai, K.. Maskell, and C.A. Johnson (eds.)]. Cambridge University Press, Cambridge, United Kingdom and New York, NY, USA, 881pp.
IPCC. (2007). Climate Change 2007: The Fourth IPCC Assessment Report. Valencia, Spain: Intergovernmental Panel on Climate Change
Jolly, M., J.M. Graham, A. Michaelis, R. Nemani and S.W. Running. 2004. A flexible, integrated system for generating meteorological surfaces derived from point sources across multiple geographic scales. Environmental modeling & software, 15: 112-121
Jonasson, S., Michelsen, A., Schmidt, I., and Nielsen, E. V. 1999. Responses in Microbes and Plants to Changed Temperature, Nutrient, and Light Regimes in the Arctic, Ecology 80: 1828–1843
Karl, T. R., C. N. Williams Jr., F. T. Quinlan, and T. A. Boden, 1990: United States Historical Climatology Network (HCN) serial temperature and precipitation data. Publ. 304, Environmental Science Division, Carbon Dioxide Information and Analysis. American Meteorological Society January 2005 | 49 Center, Oak Ridge National Laboratory, Oak Ridge, TN, 389 pp.
K-1 model developers, K-1 coupled model (MIROC) description, K-1 Technical Report, vol. 1, H. Hasumi and S. Emori (eds.), Center for Climate System Research, University of Tokyo, 34pp., 2004
Kawamitsu, Y., Yoda, S., & Agata, W. 1993. Humidity pretreatment affects the responses of stomata and CO_2 assimilation to vapor pressure difference in C3 and C4 plants. Plant Cell Physiology, 34(1), 113−11
Kimball, .S., S.W. Running, R. Nemani, 1997. An improved method for estimating surface humidity from daily minimum temperature. Ag For Met. 85:87-98.
Lal, R., 2004. Carbon sequestration in dryland ecosystems. Environ. Manage. 33, 528–544.
Lamarque, J., J. Kiehl, G. P. Brasseur, T. Butler, P. Cameron Smith, W. Collins, W. Collins, C. Granier, D. Hauglustaine, and P. Hess. 2005. Assessing future nitrogen deposition and carbon cycle feedback using a multi-model approach: analysis of nitrogen deposition. Journal of Geophysical Research 110: D19303 [Online: doi:10.1029/2005JD005825].
Luo Y., Su B., Currie W.S., et al. 2004. Progressive nitrogen limitation of ecosystem responses to rising atmospheric carbon dioxide. BioScience 54, 731–739

M. J. Menne, C. N. Williams, Jr., and R. S. Vose, 2008. United States Historical Climatology Network (USHCN) Version 2 Serial Monthly Dataset. Carbon Dioxide Information Analysis Center, Oak Ridge National Laboratory, Oak Ridge, Tennessee. [Web site] http://www.ncdc.noaa.gov/oa/climate/research/ushcn/

Ma, Z. Q., Liu, Q. J., Wang, H. M., Li, X. R., Zeng, H. Q., and Xu, W. J.: Observation and modeling of NPP for Pinus elliottii plantation in subtropical China, Sci. China Ser. D-Earth, 51, 955–965, 2008.

Mitchell, J. E. 2000. Rangeland resource trends in the United States: A technical document supporting the 2000 USDA Forest Service RPA Assessment. Gen. Tech. Rep. RMRS-GTR-68. Fort Collins, CO: U.S. Department of Agriculture, Forest Service, Rocky Mountain Research Station. 84 p.

Mooney H. A., Chu, C. 1974. Seasonal Carbon Allocation in Heteromeles arbutifolia, a California Evergreen Shrub. Oecologia, 14: 295-306

Morgan, J. A., Pataki, D. E., Körner, C., Clark, H., Del Grosso, S. J., Grünzweig, J. M., Knapp, A. K., Mosier, A. R., Newton, P. C. D., Niklaus, P. A., Nippert, J. B., Nowak, R. S., Parton, W. J., Polley, H.W. & Shaw, M. R. (2004). Water relations in grassland and desert ecosystems exposed to elevated atmospheric CO_2. Oecologia 140: 11–25.

Mu, Q., M. Zhao, S. W. Running, M. Liu, and H. Tian. 2008. Contribution of increasing CO_2 and climate change to the carbon cycle in China's ecosystems. Journal of Geophysical Research 113:G01018.

Nemani RR, Keeling CD, Hashimoto H, Jolly WM, Piper SC, Tucker CJ, Myneni RB, Running SW. 2003. Climate-driven increases in global terrestrial net primary production from 1982 to 1999. Science 300: 1560–1563

Niklaus, P. A., Spinnler, D. & Korner, C. (1998). Soil moisture dynamics of calcareous grassland under elevated CO_2. Oecologia 117: 201–208.

NOAA, NCDC. Observed Change in Annual Average Precipitation 1958 to 2008, U.S. Global Change Research Program: http://globalchange.gov/publications/reports/scientific-assessments... accessed Dec 2011.

Nozawa, T., T. Nagashima, T. Ogura, T. Yokohata, N. Okada, and H. Shiogama (2007), Climate change simulations with a coupled ocean-atmosphere GCM called the Model for Interdisciplinary Research on Climate: MIROC, CGER Supercomput. Monogr. Rep., 12, Cent. For Global Environ. Res., Natl. Inst. for Environ. Stud., Tsukuba, Japan

Owensby, C. E., J. M. Ham, A. K. Knapp, D. Bremer, and L. M. Auen. 1997. Water vapour fluxes and their impact under elevated CO2 in a C4-tallgrass prairie. Global Change Biology 3:189-195

Pacala, S., and R. Socolow (2004), Stabilization wedges: Solving the climate problem for the next 50 years with current technologies, Science, 305, 968–972.

Peek, M. S., Leffler, A. J., Hipps, L., Ivans, S., Ryel, R. J., Caldwell, M. M. 2006. Root turnover and relocation in the soil profile in response to seasonal soil water variation in a natural stand of Utah juniper (Juniperus osteosperma). Tree Physiology 26: 1469-1476

Polley, H.W., Johnson, H.B. & Derner, J.D. (2002). Soil- and plant-water dynamics in a C3/C4 grassland exposed to a subambient to superambient CO_2 gradient. Global Change Biology 8, 1118–1129.

Polley, H. W., Emmerich, W., Bradford, J. A., Sims, P. L., Johnson, D. A., Saliendra, N. Z., Svejcar, T., Angell, R., Frank, A. B., Phillips, R. L., Snyder, K. A., Morgan, J. A., Sanabria, J., Mielnick, P. C. & Dugas, W. A. (2010). Precipitation regulates the response of net ecosystem CO2 exchange to environmental variation on United States rangelands. Rangeland Ecology and Management 63, 176–18

Porporato, A., Daly, E., and Rodriguez-Iturbe, I. 2004. Soil water balance and ecosystem response to climate change. American Naturalist 164: 625–632

Porporato, A., F. Laio, L. Ridolfi, K. Caylor, and I. Rodriguez- Iturbe. 2003. Soil moisture and plant stress dynamics along the Kalahari precipitation gradient. Journal of Geophysical Research 108:4127–4134.

Reeves, M.C., J.C. Winslow, and S.W. Running, 2001. Mapping weekly rangeland vegetation productivity, Journal of Range Management, 54(suppl):A90–A105

Reeves, M.C. and J.E. Mitchell. 2010. The US Rangeland Base: A Geographic Analysis of the Extent of Coterminous US Rangelands. Submitted to: Rangeland Ecology and Management

Riera, J.L., Magnuson, J.J., Vande Castle, J.R., MacKenzie, M.D. 1998. Analysis of large scale spatial heterogeneity in vegetation indices among North American landscapes. Ecosystems 1:268- 28

Rollins, M. 2009. LANDFIRE: a nationally consistent vegetation, wildland fire and fuel assessment International Journal of Wildland Fire 18:235-249.

Running, S. W., and E. R. Hunt Jr., 1993: Generalization of a forest ecosystem process model for other biomes, BIOME–BGC, and an application for global-scale models. Scaling Physiological Processes: Leaf to Globe, edited by J. R. Ehleringer and C. B. Field, Academic Press, San Diego, 141–157.

Running, S.W. and J.C. Coughlan. 1988. A general model of forest ecosystem processes for regional applications I. Hydrologic balance, canopy gas exchange and primary production processes. Ecological Modeling

42: 125–154.

Sala, O. E., Parton, W. J., Joyce, L. A., Lauenroth, W. K. 1988. Primary production of the central grassland region of the United States. Ecology 69:40-4

Sala, O. E. et al. Global biodiversity scenarios for the year 2100. Science 287, 1770 (2000).

Svejcar, T., Mayeux, H., & Angell, R. (1997). The rangeland carbon dioxide flux project. Rangelands, 19: 16–1

Schimel, D. et al. Contribution of increasing CO2 and climate to carbon storage by ecosystems in the United States. Science 287, 2004 (2000).

Schuman GE, Janzen HH, HerrickJE. 2002. Soil carbon dynamics and potential carbon sequestration by rangelands. Environmental Pollution 116: 391-39

Schlesinger W. H., Hasey, M. M., 1981. Decomposition of Chaparral Shrub Foliage: Losses of Organic and Inorganic Constituents from Deciduous and Evergreen Leaves. Ecology, 62: 762-774

Schlesinger W.H. and Andrews J.A. 2000. Soil respiration and the global carbon cycle. Biogeochemistry 48:7-2

Shaw MR, Zavaleta ES, Chiariello NR, Cleland EE, Mooney HA, Field CB. 2002. Grassland responses to global environmental changes suppressed by elevated CO2. Science 298:1987–9

Sims, P.L., Risser, P.G., 1999. Grasslands. In: Barbour, M.G., Billings, D.W. (Eds.), North American Terrestrial Vegetation, 2nd Edition. Cambridge University Press, New York, pp. 321–354 (Chapter 9)

Solomon, S., D. Qin, M. Manning, Z. Chen, M. Marquis, K. B. Averyt, M. Tigora, and H. L. Miller, Eds., 2007. IPCC 2007. Climate Change 2007: The Physical Science Basis.

Standiford RB & Howitt RE (1993) Multiple use of California's hardwood rangelands. J. Range Manage. 46: 176-182.

Sundquist E.1993.The global carbon dioxide budget. Science 259:934-41.

Thornton, P.E., H. Hasenauer, and M.A. White, 2000 Simultaneous estimation of daily solar radiation and humidity from observed temperature and precipitation: an application over complex terrain in Austria.

Thornton, P. E., J.-F. Lamarque, N. A. Rosenbloom, and N. Mahowald. 2007, Influence of carbon-nitrogen cycle coupling on land model response to CO_2 fertilization and climate variability, Global Biogeochem. Cycles, 21, GB4018, doi:10.1029/2006GB002868

Thornton, P. K., Van de Steeg J, Notenbaert AM, Herrero M: The impacts of climate change on livestock and livestock systems in developing countries: a review of what we know and what we need to know. Agric Syst 2009, 101:113-127

Tian, H., Chen, G., Liu, M., Zhang, C., Sun, G., Lu, C., Xu, X., Ren, W., Pan, S., and Chappelka, A. 2010. Model esti tes of net primary productivity, evapotranspiration, and water use efficiency in the ter e trial cosys ems of the southern United States during 1895–2007, Forest Ecol. Manage., 2 9: 1311– 327

Turner MG, Gardner RH, O'Neil V. 1995. Ecological dynamics broad scales: ecosystems and landscapes. Bioscience 45 Su pl: S 29-35

U.S. Department of Agriculture. 1994. State soil geographic data base (STATSGO) data user's guide. Misc. Publ. No. 1492 (revised), U.S. Department of Agriculture, Soil Conservation Service, Fort Worth, Tex.

U.S. Department of Agriculture. 2009. *Summary Report: 2007 National Resources Inventory*, Natural Resources Conservation Service, Washington, DC, and Center for Survey Statistics and Methodology, Iowa State University, Ames, Iowa

Vitousek, P. M. 1994. Beyond global warming: ecology and global change. Ecology 75: 1861- 1876.

Wand, S. J. E., Midgley, G. F., Jones, M.H. & Curtis, P. S. (1999). Responses of wild C4 and C3 grass (Poaceae) species to elevated atmospheric CO_2 concentrations: a meta-analytic test of current theories and perceptions. Global Change Biology 5: 723–741.

White MA, Thornton PE, Running SW, Nemani RR. 2000. Parameterization and sensitivity analysis of the BIOME-BGC terrestrial ecosystem model: Net primary production controls.Earth Interactions 4(3):1-85

Willmott, C. J. Gaile, G.L., 1984. On the evaluation of model performance in physical geography. Spatial Statistics and Models: 443-460

Woodward F. I. 1986. Ecophysiological Studies on the Shrub Vaccinium myrtillus L. Taken from a Wide Altitudinal Range. Oecologia, 70: 580-586

Zheng D, Prince S, Wright R. 2003. Terrestrial net primary production estimates for 0.5° grid cells from field observations—a contribution to global biogeochemical modeling. Global Change Biology 9: 46–64

Appendix

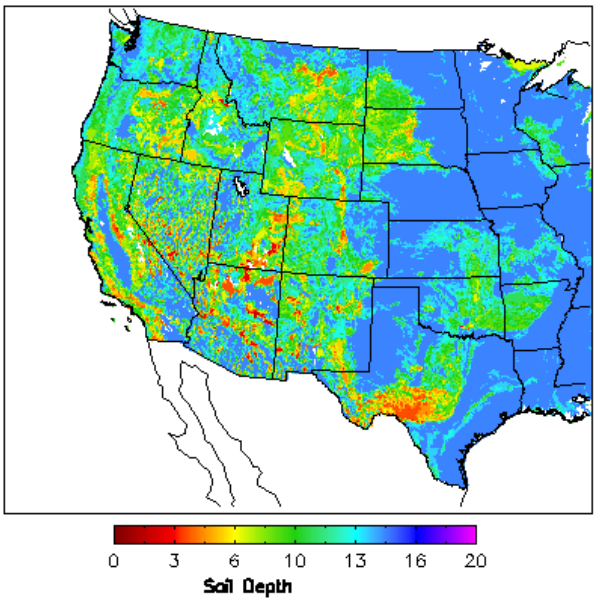

Figure A-1 Statsgo soil depth

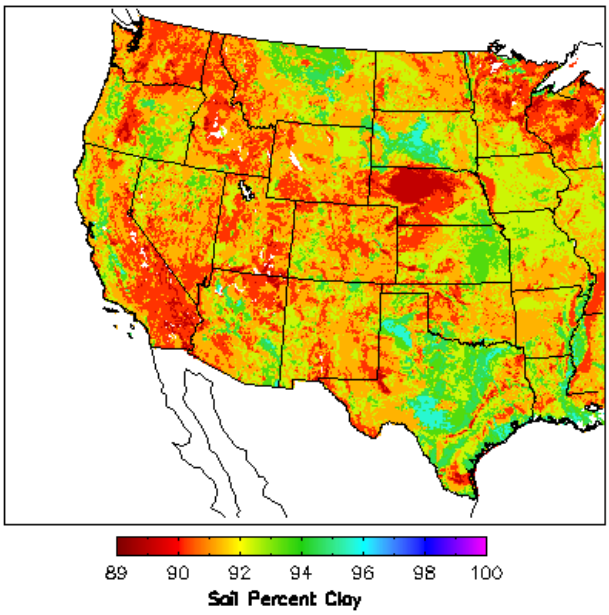

Figure A-2 Statsgo clay percentage

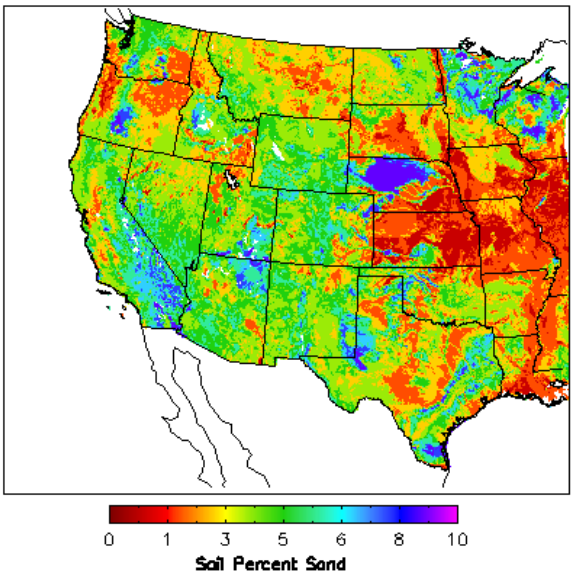

Figure A-3 Statsgo sand percentage

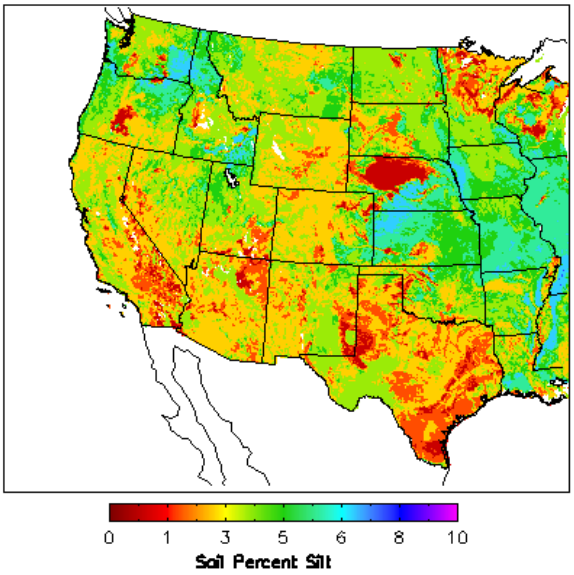

Figure A-4 Statsgo silt percentage

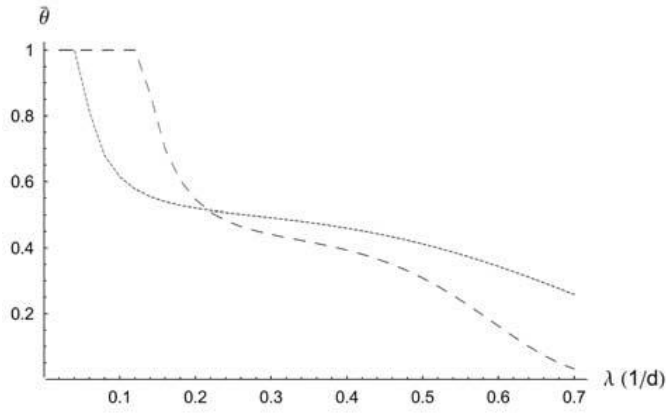

Figure A-5 Behavior of the dynamical water stress as a function of the mean rainfall rate for trees (dashed line) and grasses (dotted line). a = 1 cm, Tseas = 210 d; see text for the values of the other parameters. (Porporato 2003)

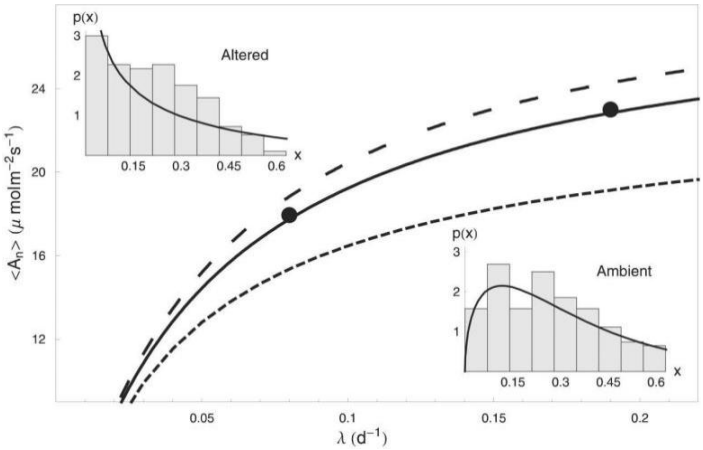

Figure A-6 Mean daily carbon assimilation rate as a function of the frequency of rainfall events for constant total amount of precipitation during a growing season. The lines are the theoretical curves derived from the soil moisture probability density function, while the two points are field data published by Knapp et al. (2002), who compared the response of a mesic grassland to ambient rainfall pattern versus an artificially increased rainfall variability. The point on the right corresponds to the ambient conditions, and the point on the left corresponds to artificially modified conditions while keeping the total rainfall the same. The continuous line is for mean total rainfall during a growing season of 507 mm, the dashed line for 600 mm, and the dotted line for 400 mm. The two insets show observed and theoretical soil moisture probability density functions for ambient and altered conditions. (Porporato 2004)

Table A-7 Original parameters used to define land cover types in Biome-BGC from White et al. (2000)

Parameter	shrub	c3	c4	Units
1 = WOODY 0 = NON-WOODY	1	0	0	Flag
1 = Use perennial Grass allocation scheme 0 = Use traditional BGC allocation	0	0	1	Flag
1 = EVERGREEN 0 = DECIDUOUS	1	0	0	Flag
1 = C3 PSN 0 = C4 PSN	1	1	0	Flag
1 = MODEL PHENOLOGY 0 = USER-SPECIFIED PHENOLOGY	1	1	1	Flag
1 = USE GDD PHENOLOGY 0 = USE STANDARD PHENOLOGY	0	0	1	Flag
Starting Gdd heat sum	0	0	0	deg. C
GDD phenology offset flag: 1 = Use killing frost offset day 0 = Use gdd heatsum offset day	0	0	1	Flag
1 = FLOWER AND USE FRUIT ALLOCATION AFTER FLOWER DAY 0 = NO FLOWER/FRUIT ALLOCATION	0	0	0	Flag
photosynthetic stem	0	0	0	Flag
0 = No Fruit Litterfall, use only disturbance handler, 1 = reset fruit C to zero on first day of year (old agro bgc behavior), 2 = use a litterfall period (without dead fruit pool)	0	0	0	Flag
0 = Use proportion of Senescence period to end litterfall, 1=end litterfall at beginning of next growing season	1	1	1	Flag
yearday to start new growth (jan. 1 = 0) when phenology flag = 0) (doy 335 with jan. 1 = doy 1) (apr. 1 = 90)	0	0	120	yday
yearday to end litterfall (when phenology flag = 0) (nov 8 = 311 for last harvest)	0	364	364	yday
yearday for flowering, if flower flag and user specified phenology	0	200	200	yday
transfer growth period as fraction of growing season	0.3 White et.al. 2000	1	0.6	prop.
senescence period as fraction of growing season (if not using gdd phenology)	0.45 White et.al. 2000	0.45	0.45	prop.
litterfall period as a fraction of senescence period. Should be >= 1.0	4.2 White et.al. 2000	1	2	prop.
annual leaf and fine root turnover fraction (and stem for perennial grass)	0.32 White et.al. 2000	1	1	1/yr
annual live wood turnover fraction (for perennial grass affects coarse root turnover only)	0.7 White et.al. 2000	0	0.25	1/yr
annual whole-plant mortality fraction	0.02 White et.al. 2000	0.1	0.1	1/yr
(ALLOCATION) new fine root C : new leaf C	1.4 White et.al. 2000	1	0.5	ratio
(ALLOCATION) new stem C : new leaf C	0.22 White et.al. 2000	0	0.285	ratio
(ALLOCATION) new live wood C : new total wood C	1 White et.al. 2000	1	1	ratio
(ALLOCATION) new croot C : new stem C	0.29 White et.al. 2000	0	1.3	ratio
(ALLOCATION) current growth proportion	0.5 White et.al. 2000	0.5	0.68	prop.
C:N of leaves	35 White et.al. 2000	35	61.5	kgC/KgN

C:N of leaf litter	75 White et.al. 2000	35	93.4	kgC/KgN
C:N of fine roots	58 White et.al. 2000	50	65.6	kgC/KgN
C:N of coarse roots	65.6 White et.al. 2000	65.6	65.6	kgC/KgN
C:N of dead coarse roots	65.6 White et.al. 2000	65.6	65.6	kgC/KgN
C:N of live wood	50 White et.al. 2000	0	111.6	kgC/KgN
C:N of dead wood	730 White et.al. 2000	0	118.8	kgC/KgN
leaf litter labile proportion	0.56 White et.al. 2000	0.68	0.43	prop.
leaf litter cellulose proportion	0.29 White et.al. 2000	0.23	0.45	prop.
leaf litter lignin proportion	0.15 White et.al. 2000	0.09	0.12	prop.
fine root labile proportion	0.34 White et.al. 2000	0.34	0.5	prop.
fine root cellulose proportion	0.44 White et.al. 2000	0.44	0.33	prop.
fine root lignin proportion	0.22 White et.al. 2000	0.22	0.17	prop.
dead stem labile proportion	0 White et.al. 2000	0.125	0.25	prop.
dead wood cellulose proportion	0.29 White et.al. 2000	0.75	0.33	prop.
dead wood lignin proportion	0.71 White et.al. 2000	0.125	0.42	prop.
canopy water interception coefficient	0.045 White et.al. 2000	0.021	0.022	1/LAI/d
canopy light extinction coefficient	0.55 White et.al. 2000	0.48	0.33	
all-sided to projected leaf area ratio	2.3 White et.al. 2000	2	2	ratio
canopy average specific leaf area	12 White et.al. 2000	49	24.7	m^2/kgC
ratio of shaded SLA:sunlit SLA	2 White et.al. 2000	2	2	ratio
fraction of leaf N in Rubisco	0.04 White et.al. 2000	0.15	0.1	prop.
fraction of leaf N in PEP Carboxylase	0.03 White et.al. 2000	0	0.04	prop.
maximum stomatal conductance	0.003 White et.al. 2000	0.005	0.006	m/s
cuticular conductance	0.00001 White et.al. 2000	0.00001	0.00006	m/s
boundary layer conductance	0.08 White et.al. 2000	0.04	0.04	m/s
leaf water potential: start of conductance reduction	-0.81 White et.al. 2000	-0.73	-0.73	Mpa
leaf water potential: complete conductance reduction	-4.2 White et.al. 2000	-2.7	-3.5	Mpa
vapor pressure deficit: start of conductance reduction	970 White et.al. 2000	1000	1000	Pa
vapor pressure deficit: complete conductance reduction	4100 White et.al. 2000	5000	5000	Pa
Annual such that retranslocation and storage do not occur, and cpool and npool are harvested if GDD phenology with harvest is used; 1 = yes, 0 = no	0	0	0	Flag
Seed Carbon	0	0	0	kgc/m^2/yr
Fruit C:N	0	0	30.4	kgC/KgN
Allocation of carbon to fruit after flowering date	0	0	1.2	prop.
Critical soil temperature for leaf onset	12	12	12	deg. C
GDD Base	10	10	10	deg. C
GDD Min	7.3	7.3	7.3	deg. C
GDD Max	40	40	40	deg. C
gdd emergance	0	0	0	deg. C
GDD start of stem elongation	375	375	375	deg. C
GDD Flower	925	925	925	deg. C
GDD offset	1750	1750	1750	deg. C

Table A-8 Calibrated parameters used to define land cover types in Biome-BGC

Parameter	Shrub	c3	c4	Units
1 = WOODY 0 = NON-WOODY	1	0	0	Flag
1 = Use perennial Grass allocation scheme 0 = Use traditional BGC allocation	0	0	1	Flag
1 = EVERGREEN 0 = DECIDUOUS	1	0	0	Flag
1 = C3 PSN 0 = C4 PSN	1	1	0	Flag
1 = MODEL PHENOLOGY 0 = USER-SPECIFIED PHENOLOGY	1	1	1	Flag
1 = USE GDD PHENOLOGY 0 = USE STANDARD PHENOLOGY	0	0	1	Flag
Starting Gdd heat sum	0	0	0	deg. C
GDD phenology offset flag: 1 = Use killing frost offset day 0 = Use gdd heatsum offset day	0	0	1	Flag
1 = FLOWER AND USE FRUIT ALLOCATION AFTER FLOWER DAY 0 = NO FLOWER/FRUIT ALLOCATION	0	0	0	Flag
photosynthetic stem	0	0	0	Flag
0 = No Fruit Litterfall, use only disturbance handler, 1 = reset fruit C to zero on first day of year (old agro bgc behavior), 2 = use a litterfall period (without dead fruit pool)	0	0	0	Flag
0 = Use proportion of Senescence period to end litterfall, 1=end litterfall at beginning of next growing season	1	1	1	Flag
yearday to start new growth (jan. 1 = 0) when phenology flag = 0) (doy 335 with jan. 1 = doy 1) (apr. 1 = 90)	0	0	120 Di Vittorio 2010	yday
yearday to end litterfall (when phenology flag = 0) (nov 8 = 311 for last harvest)	0	364 White et.al. 2000	364 Di Vittorio 2010	yday
yearday for flowering, if flower flag and user specified phenology	0	200 White et.al. 2000	200 Di Vittorio 2010	yday
transfer growth period as fraction of growing season	0.3 White et.al. 2000	1 White et.al. 2000	0.6 Di Vittorio 2010	prop.
senescence period as fraction of growing season (if not using gdd phenology)	0.45 White et.al. 2000	0.45 White et.al. 2000	0.45 Di Vittorio 2010	prop.
litterfall period as a fraction of senescence period. Should be >= 1.0	4.2 White et.al. 2000	1 White et.al. 2000	2 Di Vittorio 2010	prop.
annual leaf and fine root turnover fraction (and stem for perennial grass)	0.16 (calibrated) Peek 2006	1 White et.al. 2000	1 Di Vittorio 2010	1/yr
annual live wood turnover fraction (for perennial grass affects coarse root turnover only)	0.7 White et.al. 2000	0 White et.al. 2000	0.25 Di Vittorio 2010	1/yr
annual whole-plant mortality fraction	0.01 White et.al. 2000	0.1 White et.al. 2000	0.1 Di Vittorio 2010	1/yr
(ALLOCATION) new fine root C : new leaf C	2.5 (calibrated) Mooney 1974	1 White et.al. 2000	0.5 Di Vittorio 2010	ratio
(ALLOCATION) new stem C : new leaf C	0.145 (calibrated) Mooney 1974	0 White et.al. 2000	0.285 Di Vittorio 2010	ratio
(ALLOCATION) new live wood C : new total wood C	0.5 (calibrated) Mooney 1974	1 White et.al. 2000	1 Di Vittorio 2010	ratio
(ALLOCATION) new croot C : new stem C	0.29 White et.al. 2000	0 White et.al. 2000	1.3 Di Vittorio 2010	ratio
(ALLOCATION) current growth proportion	0.5 (calibrated) No Lit	0.5 White et.al. 2000	0.68 Di Vittorio 2010	prop.
C:N of leaves	70 (calibrated) Schlesinger 1981	35 White et.al. 2000	61.5 Di Vittorio 2010	kgC/KgN
C:N of leaf litter	150 (calibrated) Enriquez 1993	35 White et.al. 2000	93.4 Di Vittorio 2010	kgC/KgN
C:N of fine roots	58 (calibrated) Gordon 2000	50 White et.al. 2000	65.6 Di Vittorio 2010	kgC/KgN

C:N of coarse roots	65.6 White et.al. 2000	65.6 White et.al. 2000	65.6 Di Vittorio 2010	kgC/KgN
C:N of dead coarse roots	65.6 White et.al. 2000	65.6 White et.al. 2000	65.6 Di Vittorio 2010	kgC/KgN
C:N of live wood	50 White et.al. 2000	0 White et.al. 2000	111.6 Di Vittorio 2010	kgC/KgN
C:N of dead wood	730 White et.al. 2000	0 White et.al. 2000	118.8 Di Vittorio 2010	kgC/KgN
leaf litter labile proportion	0.56 White et.al. 2000	0.68 White et.al. 2000	0.43 Di Vittorio 2010	prop.
leaf litter cellulose proportion	0.29 White et.al. 2000	0.23 White et.al. 2000	0.45 Di Vittorio 2010	prop.
leaf litter lignin proportion	0.15 White et.al. 2000	0.09 White et.al. 2000	0.12 Di Vittorio 2010	prop.
fine root labile proportion	0.34 White et.al. 2000	0.34 White et.al. 2000	0.5 Di Vittorio 2010	prop.
fine root cellulose proportion	0.44 White et.al. 2000	0.44 White et.al. 2000	0.33 Di Vittorio 2010	prop.
fine root lignin proportion	0.22 White et.al. 2000	0.22 White et.al. 2000	0.17 Di Vittorio 2010	prop.
dead stem labile proportion	0 White et.al. 2000	0.125 White et.al. 2000	0.25 Di Vittorio 2010	prop.
dead wood cellulose proportion	0.29 White et.al. 2000	0.75 White et.al. 2000	0.33 Di Vittorio 2010	prop.
dead wood lignin proportion	0.71 White et.al. 2000	0.125 White et.al. 2000	0.42 Di Vittorio 2010	prop.
canopy water interception coefficient	0.0001 White et.al. 2000	0.021 White et.al. 2000	0.022 Di Vittorio 2010	1/LAI/d
canopy light extinction coefficient	0.55 White et.al. 2000	0.48 White et.al. 2000	0.33 Di Vittorio 2010	
all-sided to projected leaf area ratio	2.3 White et.al. 2000	2 White et.al. 2000	2 Di Vittorio 2010	ratio
canopy average specific leaf area	4 Ackerly 2002	49 White et.al. 2000	24.7 Di Vittorio 2010	m^2/kgC
ratio of shaded SLA:sunlit SLA	2 White et.al. 2000	2 White et.al. 2000	2 Di Vittorio 2010	ratio
fraction of leaf N in Rubisco	.16 (calibrated) Ellsworth 2004	0.15 White et.al. 2000	0.1 Di Vittorio 2010	prop.
fraction of leaf N in PEP Carboxylase	0.03 White et.al. 2000	0 White et.al. 2000	0.04 Di Vittorio 2010	prop.
maximum stomatal conductance	0.002 (calibrated) Woodward 1986	0.005 White et.al. 2000	0.006 Di Vittorio 2010	m/s
cuticular conductance	0.00001 White et.al. 2000	0.000 White et.al. 200001	0.00006 Di Vittorio 2010	m/s
boundary layer conductance	0.08 White et.al. 2000	0.04 White et.al. 2000	0.04 Di Vittorio 2010	m/s
leaf water potential: start of conductance reduction	-0.81 White et.al. 2000	-0.73 White et.al. 2000	-0.73 Di Vittorio 2010	Mpa
leaf water potential: complete conductance reduction	-4.2 White et.al. 2000	-2.7 White et.al. 2000	-3.5 Di Vittorio 2010	Mpa
vapor pressure deficit: start of conductance reduction	970 White et.al. 2000	1000 White et.al. 2000	1000 Di Vittorio 2010	Pa
vapor pressure deficit: complete conductance reduction	4100 White et.al. 2000	5000 White et.al. 2000	5000 Di Vittorio 2010	Pa
Annual such that retranslocation and storage do not occur, and cpool and npool are harvested if GDD phenology with harvest is used; 1 = yes, 0 = no	0	0 White et.al. 2000	0 Di Vittorio 2010	Flag
Seed Carbon	NA	0 White et.al. 2000	0 Di Vittorio 2010	kgc/m^2/yr
Fruit C:N	NA	0 White et.al. 2000	30.4 Di Vittorio 2010	kgC/KgN
Allocation of carbon to fruit after flowering date	NA	0 White et.al. 2000	1.2 Di Vittorio 2010	prop.
Critical soil temperature for leaf onset	NA	12 White et.al. 2000	12 Di Vittorio 2010	deg. C
GDD Base	NA	NA	10 Di Vittorio 2010	deg. C
GDD Min	NA	NA	7.3 Di Vittorio 2010	deg. C
GDD Max	NA	NA	40 Di Vittorio 2010	deg. C
gdd emergance	NA	NA	0 Di Vittorio 2010	deg. C
GDD start of stem elongation	NA	NA	375 Di Vittorio 2010	deg. C
GDD Flower	NA	NA	925 Di Vittorio 2010	deg. C
GDD offset	NA	NA	1750 Di Vittorio 2010	deg. C

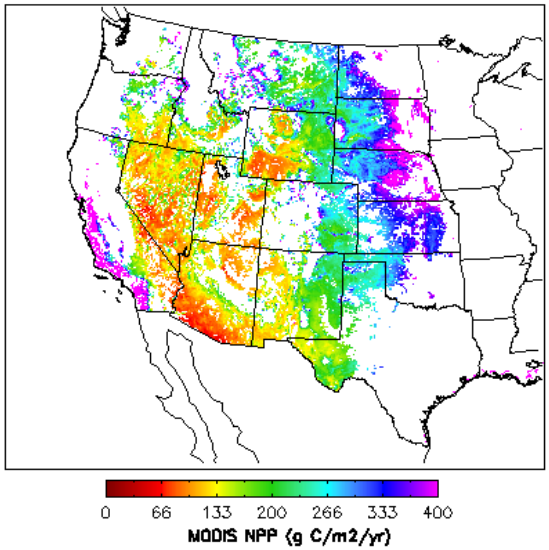

Figure A-9 MODIS average annual NPP from 2000-2009 (g C/m^2/year).

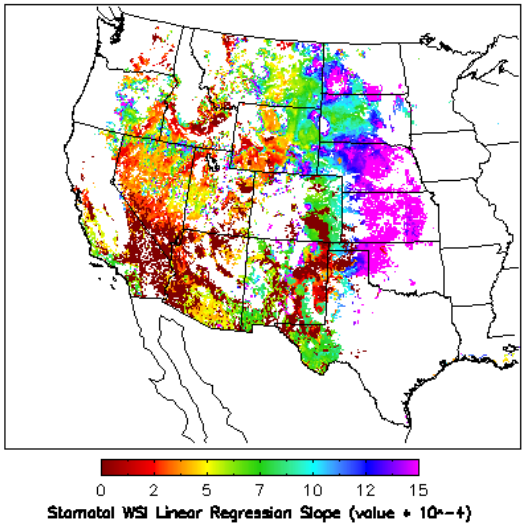

Figure A-10 WSI linear regression slope (value *10-4) of Biome-BGC simulation data from 2001-2100.

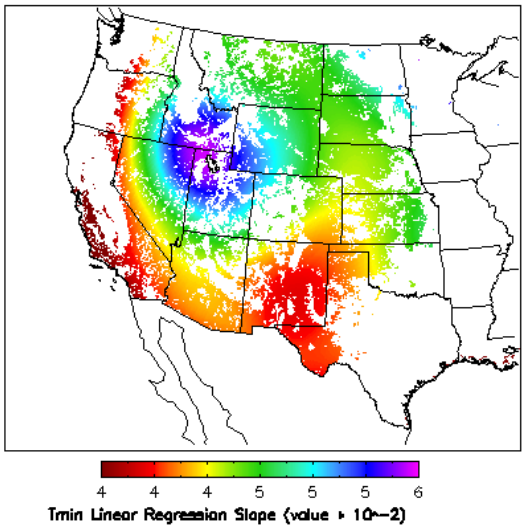

Figure A-11 Tmin linear regression slope (values * 10-2) of Miroc3.2 GCM data from 2001-2100.

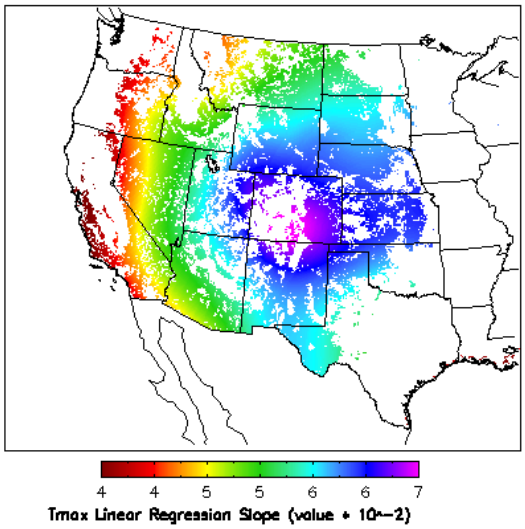

Figure A-12 Tmax linear regression slope (values * 10-2) of Miroc3.2 GCM data from 2001-2100.

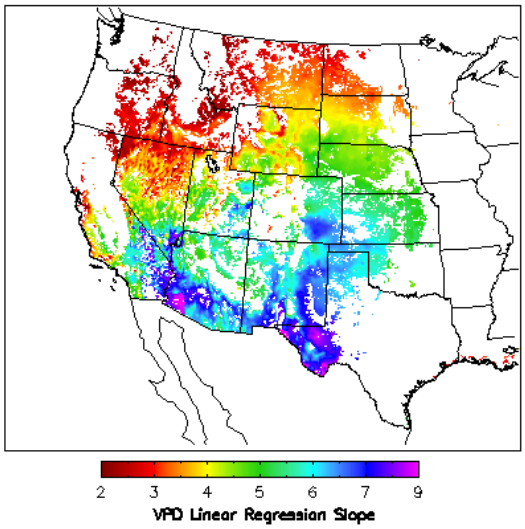

Figure A-13 VPD linear regression slope of data from 2001-2100.

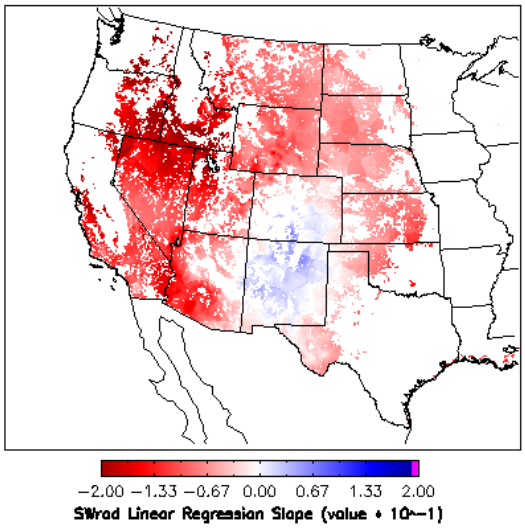

Figure A-14 Solar radiation linear regression slope (value * 10^-1) of data from 2001-2100.

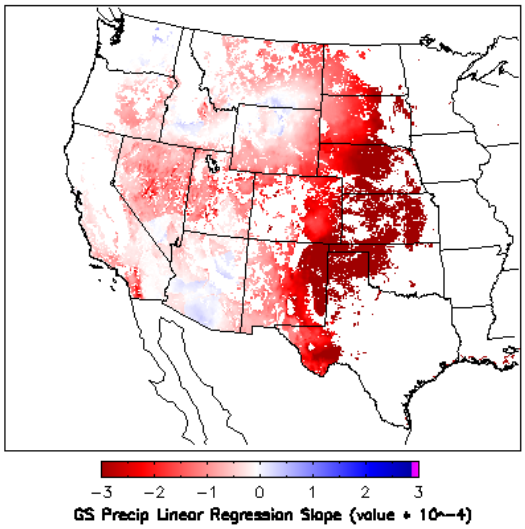

Figure A-15 Growing season precipitation linear regression slope values *10-4 of Miroc3.2 GCM data from 2001-2100.

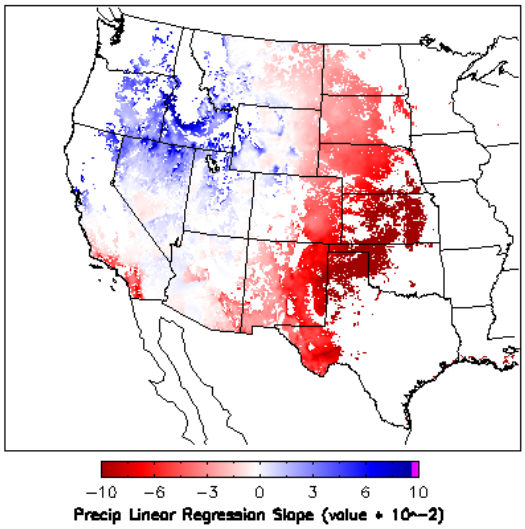

Figure A-16 Annual precipitation linear regression slope (value * 10^-2) of Miroc3.2 GCM data from 2001-2100.

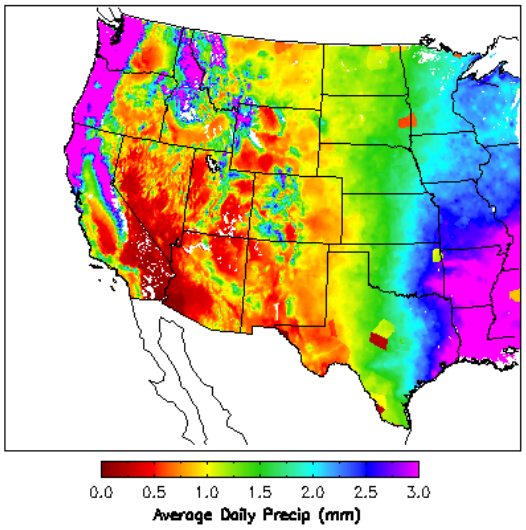

Figure A-17 Avg daily precipitation (mm) of Miroc3.2 GCM data from 2001-2100.

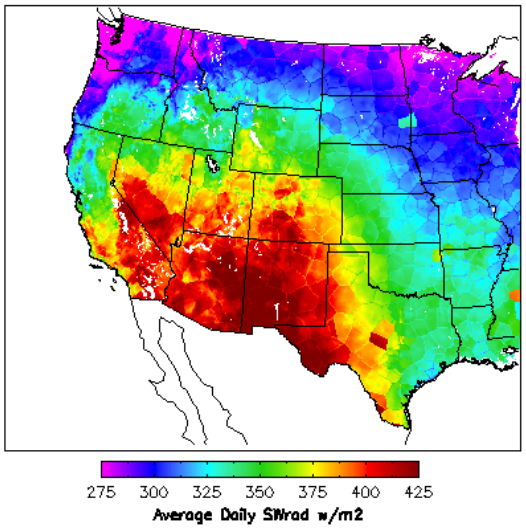

Figure A-18 Avg daily Solar radiation (w/m^2) from 2001-2100.

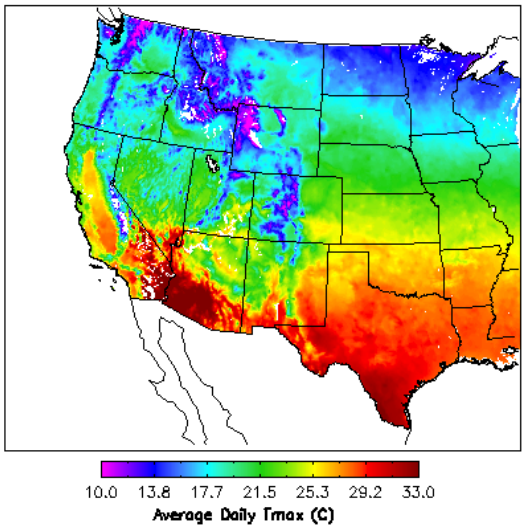

Figure A-19 Avg daily tmax (C) of Miroc3.2 GCM data from 2001-2100.

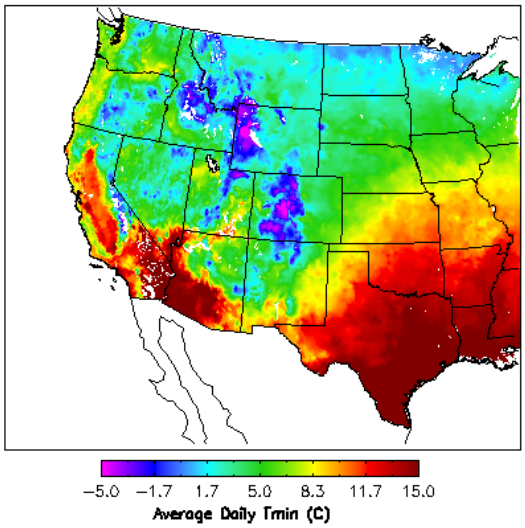

Figure A-20 Avg daily tmin (C) of Miroc3.2 GCM data from 2001-2100.

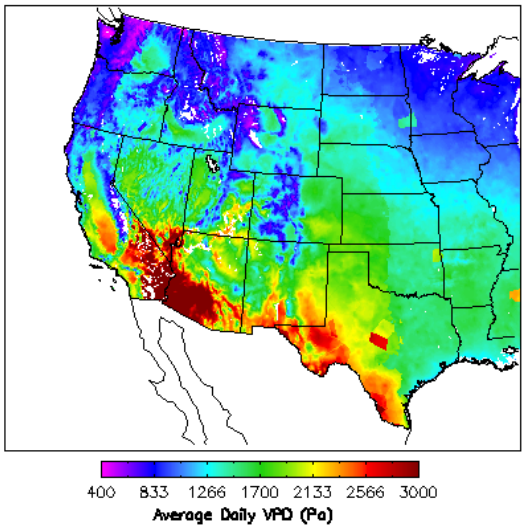

Figure A-21 Avg daily VPD (Pa) from 2001-2100.

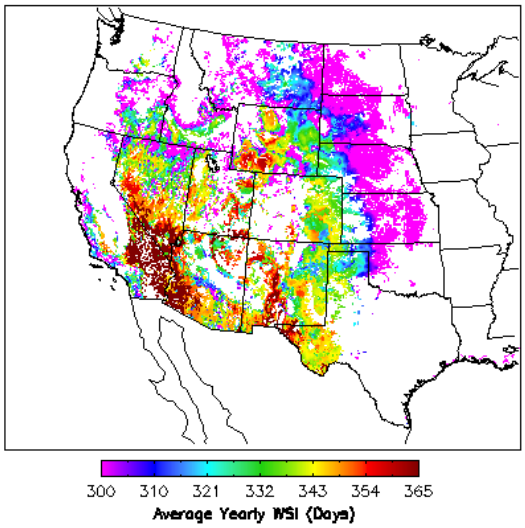

Figure A-22 Water stress index 100 year yearly avg in days. Days of water stress = sum(daily(m_vpd * m_psi)).

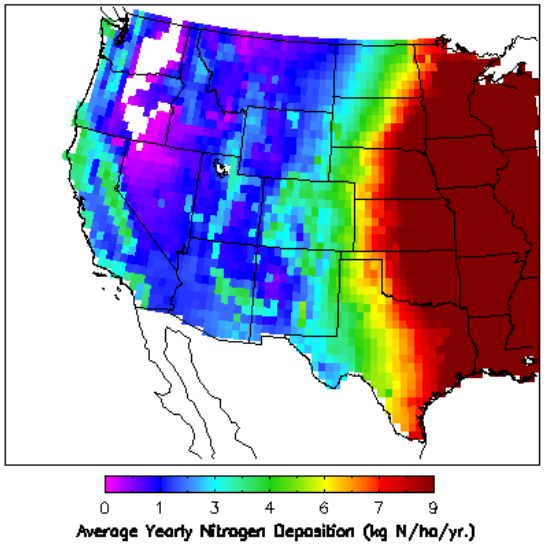

Figure A-23 Average yearly nitrogen deposition for year 2001 (kg N/ha/yr.). Every year of simulation maintained this pattern and changed every decade at a rate determined by Table A-24.

Table A-24 IPCC CO2 emissions scenarios and their corresponding NOx emissions (TgN/yr) (IPCC 2001) by decade along with each decades rate of increase as compared to the 2000-2009 decade for A1B.

Year	A1B	A1T	A1FI	A2	B1	B2	A1p	A2p	B1p	B2p	IS92a
2000	32	32	32	32	32	32	32.5	32.5	32.5	32.5	37
2010	39.3	38.8	39.7	39.2	36.1	36.7	41	39.6	34.8	37.6	43.4
2020	46.1	46.4	50.4	50.3	39.9	42.7	48.9	50.7	39.3	43.4	49.8
2030	50.2	55.9	62.8	60.7	42	48.9	52.5	60.8	40.7	48.4	55.2
2040	48.9	59.7	77.1	65.9	42.6	53.4	50.9	65.8	44.8	52.8	59.6
2050	47.9	61	94.9	71.1	38.8	54.5	49.3	71.5	48.9	53.7	64
2060	46	59.6	102.1	75.5	34.3	56.1	47.2	75.6	48.9	55.4	67.8
2070	44.2	51.7	108.5	79.8	29.6	56.3	45.1	80.1	48.9	55.6	71.6
2080	42.7	42.8	115.4	87.5	25.7	59.2	43.3	87.3	48.9	58.5	75.4
2090	41.4	34.8	111.5	98.3	22.2	60.9	41.8	97.9	41.2	60.1	79.2
2100	40.2	28.1	109.6	109.2	18.7	61.2	40.3	109.7	33.6	60.4	83

Rate of Increase
0
0.228125
0.440625
0.56875
0.528125
0.496875
0.4375
0.38125
0.334375
0.29375
0.25625